bioRχiv
THE PREPRINT SERVER FOR BIOLOGY

***bioRxiv***, 2024, 1–16

doi: xx.xxxx/xxxx

PAPER

# Deep sequencing of 16 *Ixodes ricinus* ticks unveils insights into their interactions with endosymbionts.

Paulina M. Lesiczka[1, *§], Tal Azagi[2,*], Aleksandra I. Krawczyk[2,¶], William T. Scott, Jr.[3,4], Ron P. Dirks[5], Ladislav Šimo[6], Gerhard Dobler[7], Bart Nijsse[3,4], Peter J. Schaap[3,4], Hein Sprong[2†] and Jasper J. Koehorst[3,4,‡]

[1]Department of Veterinary Sciences, Faculty of Agrobiology, Food and Natural Resources, Czech University of Life Sciences, Prague, Czech Republic and [2]Centre for Infectious Diseases (CIb), National Institute for Public Health and the Environment (RIVM), 3720 BA Bilthoven, Netherlands and [3]Laboratory of Systems and Synthetic Biology, Wageningen University & Research, 6708 PB Wageningen, The Netherlands and [4]UNLOCK, Wageningen University, 6708 PB Wageningen, The Netherlands and [5]Future Genomics Technologies BV, 2333 BE Leiden, The Netherlands and [6]Anses INRAE, Ecole Nationale Vétérinaire d'Alfort, UMR BIPAR, Laboratoire de Santé Animale, 94700, Maisons-Alfort, France and [7]Bundeswehr Institute of Microbiology, Neuherbergstraße 11, 80937 München, Germany

[**]Present address: Centre for Monitoring of Vectors (CMV), Netherlands Institute for Vectors, Invasive plants and Plant health (NIVIP), Netherlands Food and Consumer Product Safety Authority (NVWA), Wageningen, the Netherlands
[††]Present address: Mitrani Department of Desert Ecology, The Swiss Institute for Dryland Environmental and Energy Research, The Jacob Blaustein Institutes for Desert Research, Ben-Gurion University of the Negev, Midreshet Ben-Gurion, Israel
[*] These two authors contributed equally to this work.
[†] Corresponding author biology: hein.sprong@rivm.nl
[‡] Corresponding author bioinformatics: jasper.koehorst@wur.nl

## Abstract

**Background:** *Ixodes ricinus* ticks act as vectors for numerous pathogens that present substantial health threats. Additionally, they harbor vertically transmitted symbionts, some of which have been linked to diseases. The difficulty of isolating and cultivating these symbionts has has hampered our understanding of their biological role, their potential to cause disease, and their modes of transmission. To expand our understanding on the tick symbiont *Midichloria mitochondrii* and on *Rickettsia helvetica*, which has been linked to disease in humans, we utilized deep sequencing on sixteen individual adult female ticks. Among these, eight were collected from a coastal sand dune environment, while another eight were obtained from forested areas in the Netherlands.
**Results:** By employing a combination of next-generation and third-generation sequencing techniques, we successfully reconstructed the complete genomes of *M. mitochondrii* from eleven individuals, *R. helvetica* from eight individuals and the mitochondrial genome from all ticks. Additionally, we visualised the location of *R. helvetica* in tick organs and constructed genome-scale metabolic models (GEMs) of both symbionts to study their growth related environmental dependencies.
Our analysis revealed a strong cophylogeny between *M. mitochondrii* and mitochondrial genomes, suggesting frequent maternal transmission. In contrast, the absence of cophylogeny between *R. helvetica* and the mitochondrial genomes, coupled with its presence in the *receptaculum seminis* of *I. ricinus* females, raises the possibility of paternal transmission of *R. helvetica*.
Notably, the genetic diversity of *R. helvetica* was found to be very low, except for the *rick*A virulence gene, where the presence of up to thirteen insertions of a 33nt-long repeat led to significant variability. However, this variation could not account for the differences in infection prevalence observed across eight distinct locations in the Netherlands.
**Conclusions:** By employing deep sequencing, it becomes feasible to extract complete genomes and genetic data of symbionts directly from their host organisms. This methodology serves as a robust means to gain fresh insights into their interactions. Our observations, which suggest paternal transmission of *R. helvetica*, a relatively unexplored mode of transmission in ticks, require validation through experimental investigations. The genetic variations identified in the *rick*A virulence gene of *R. helvetica* have the potential to influence the infectivity and transmission dynamics of *R. helvetica*.

**Key words**: *Ixodes ricinus*, Deep Sequencing, Endosymbionts, Genome Reconstruction, *Midichloria mitochondrii*, *Rickettsia helvetica*, Genome-scale metabolic modeling, Cophylogenetic analysis, Paternal Transmission

**Compiled on:** April 22, 2024.

## Background

*Ixodes ricinus*, the most common tick species in the Palearctic realm, carries a variety of facultative symbionts, some of which can cause infectious diseases in humans (hereafter referred to as pathogens). The most common tick-borne diseases associated with *I. ricinus* are Lyme disease (LB) which is caused by *Borrelia burgdorferi sensu lato* and tick-borne encephalitis (TBE), which is caused by tick-borne encephalitis virus [1]. In addition, *I. ricinus* transmits several emerging pathogens such as *Rickettsia helvetica*, *Anaplasma phagocytophilum*, *Borrelia miyamotoi*, *Neoehrlichia mikurensis*, and several *Babesia* species [2]. Infections with these pathogens have been associated with human disease in cross-sectional and case studies, but their pathogenic potential has not been fully understood [3, 4]. While many aspects of agents causing LB and TBE are extensively studied, emerging tick-borne pathogens, as well as their non-pathogenic symbionts, have received less attention. These microorganisms can influence the tick host's metabolism, development, reproduction, stress defense, and immunity [5], and may indirectly contribute to the transmission dynamics of tick-borne pathogens, significantly impacting human and animal health [6]. The biological role, virulence, and transmission dynamics of tick symbionts and some of the pathogens are often difficult to study due to challenges in isolating and culturing them. A notable example is *Midichloria mitochondrii*, initially discovered in the ovaries of ticks. *M. mitochondrii* has been found to be highly prevalent in various tissues of *I. ricinus* [7, 8, 9, 10]. Since its discovery, *Midichloria* symbionts have been detected in several tick species across different genera, albeit with varying prevalence [11], and are believed to contribute to detoxification, vitamin supply, and energy-related functions, based on their observed interactions and effects within host cells [12]. While *M. mitochondrii* has not been associated with human disease and is only considered in the context of tick-symbiont interactions, other tick symbionts such as *Rickettsia helvetica* cannot be so clearly defined. *Rickettsia helvetica* is a Gram-negative, obligate intracellular bacterium formerly included in the Spotted Fever Group Rickettsiae (SFGR) [13]. *Rickettsia helvetica* can be transmitted by tick bites and has been associated with human disease. Only a few human cases have been reported in Europe [14, 15, 16, 17, 18, 19] and detection in cerebrospinal fluid of suspected Lyme neuroborreliosis patients has been shown in the Netherlands and Denmark. However, it is unclear whether the infection with *R. helvetica* can cause disease or might change the course of Lyme disease [20, 21]. Moreover, studies on the involvement of *R. helvetica* in sarcoidosis seem to be contradictory [22]. Thus, the extent of *R. helvetica*'s infectivity and pathogenicity is still under investigation, and little is known about its ecoepidemiology [23, 24]. DNA of *R. helvetica* has only been sporadically detected in wildlife [25, 26, 27, 28, 29] with no clear animal reservoir. This symbiont is transmitted vertically from one generation of ticks to the next and has been repeatedly isolated from questing *I. ricinus* in European countries [30], which are currently thought to be the main reservoir for *R. helvetica* in nature [25]. *Rickettsia helvetica* infection rates in *I. ricinus* vary from 0% to 66% [25], resulting in highly variable human exposure from tick bites. The reason for this high variability is unknown and could be attributed to the capacity of *R. helvetica* to be beneficial for the tick host under certain environmental conditions [31] or it could be related to genetic variation within *R. helvetica* populations, but the latter has not been investigated so far.

The pathogenic potential of *R. helvetica* has been explored, to a certain extent, on the cellular level. While other rickettsial species, which are pathogenic to humans, utilise actin-based cell-to-cell motility [32], a culture of *R. helvetica* has been shown to lack this ability in vitro [24], possibly due to a deletion in the gene encoding sca2, a protein required for virulence that stimulates actin filament assembly [33, 34]. In addition, although the sequence encoding the RickA protein, a bacterial actin nucleator [35], was complete, its expression was apparently insufficient to enable actin-based motility in the strains studied [24]. Comparative analyses of its genetic makeup and metabolic potential are needed to clarify the pathogenic potential of *R. helvetica* as well as its interaction and localization within the tick host.

Studies of tick microbial endosymbionts began with sequencing fragments of the 16S rRNA gene or targeting specific genes involved in metabolic pathways [36]. With the advancement of sequencing technologies that enabled the generation of endosymbiont genomes [37, 38], recent studies have shifted to whole-genome comparisons and a more thorough exploration of metabolic co-dependencies in tick-symbiont relationships [39, 40, 41]. Furthermore, thanks to deep sequencing technologies, the number of available tick genomes is increasing over the past years [42, 43, 44], and recently the first fully annotated genome of *Ixodes scapularis* was published [45]. The data obtained directly from Ixodes scapularis yielded an improved whole genome of the endosymbiont *Rickettsia buchneri* without the need for bacterial culture, which can be particularly time and resource consuming for intracellular bacteria [46]. Thus, by obtaining high-quality genetic data directly from tick samples, it seems increasingly possible to simultaneously study in depth the tick host and all of its bacterial tenants, referred to as the tick holobiont, in depth and potentially uncover the underlying genetic mechanisms that form the basis for their interactions.

Advances in sequencing technologies have ushered in a new era of understanding by enabling the comprehensive annotation of complete tick mitochondrial genomes (mt genomes). These genomic insights have significantly enriched our understanding of tick phylogeny, population genetics, and evolutionary processes [47, 48]. Given ticks' intimate association with symbiotic microbes crucial for their hematophagous lifestyle [49], the incorporation of mt genomes into co-phylogeny analyses presents a promising avenue for unraveling the evolutionary patterns of tick symbionts [50] . This approach holds particular significance for symbionts like *M. mitochondrii* which inhabit tick mitochondria [51] offering a unique window into their evolutionary trajectory.

Genome-scale model (GEM) reconstruction and analysis can further enhance this understanding by detailing the metabolic interactions and dependencies between ticks and their symbionts. These models can elucidate how these endosymbionts may contribute to the metabolic network, revealing potential targets for controlling tick populations and preventing tick-borne diseases. Additionally, GEMs can provide insights into the co-evolutionary dynamics of ticks and their symbionts, as has been shown in recent works [52], offering a clearer picture of how these complex biological systems have adapted and evolved together over time.

In this study, we applied deep sequencing on sixteen *Ixodes ricinus* specimens to unveil the genetic variation and differences in transmission dynamics of *M. mitochondrii* and *R. helvetica*. Complete genomes were obtained directly from the individual ticks using a hybrid assembly approach combining PromethION and Illumina sequencing. In addition to interspecies whole genome comparisons, we determined the genetic association of *R. helvetica* and *M. mitochondrii* with their tick hosts to draw conclusions about the mode of transmission of these symbionts. To further our understanding of the latter, we visualised *R. helvetica* in tick organs. Finally, we identified (potential) metabolic pathways within *Rickettsia* and *Midichloria* species that could complement essential metabolic functions in ticks.

## Materials and Methods

### 2.1 Tick biospecimen metadata, molecular detection of *R. helvetica*, sequencing and Data FAIRification

***Tick sample metadata and processing***

Lab-reared: Two questing *I. ricinus* nymphs were collected in September 2020 by blanket dragging in "De Dorschkamp", a deciduous forest east of Wageningen, the Netherlands (51°58'39.5"N, 5°41'59.3"E) (Table 1). Nymphs were morphologically identified to species level using an identification key [53]. To obtain adult *I. ricinus*, the nymphs were fed on an artificial membrane blood feeding system, as described in [54]. These two engorged nymphs were collected from the feeding membrane and incubated at room temperature until they moulted to adults, which were subsequently stored at -80°C. We designated *I. ricinus* adult female #1 as biospecimen Lab_F1 (F1) and *I. ricinus* adult female #2 as biospecimen Lab_F2 (F2).

Field samples: Fourteen *I. ricinus* adult females were collected. Six questing *I. ricinus* adult females were collected by blanket dragging in March 2022 in "De Dorschkamp", a forested (f) area in the Netherlands and designated as biospecimens: Ir_f1, Ir_f3, Ir_f6, Ir_11, Ir_f12, Ir_f16. In addition, eight questing *I. ricinus* adult females were collected in September 2021 by blanket dragging in "De Amsterdamse Waterleiding Duinen", a coastal sand dune area (d) in the Netherlands (52°32'79.9"N, 4°54'38.6"E). These samples were designated as biospecimens Ir_d1, Ir_d2, Ir_d3, Ir_d4, Ir_d5, Ir_d6, Ir_d7, Ir_d9. All ticks were kept at -80°C until further processing.

***Molecular detection of R. helvetica and analyses of the rickA gene***

Questing nymphs were collected in Duin & Kruidberg, the Netherlands (52°18'13.5"N 4°31'59.5"E) on 14.08.2018. Samples were also collected in Schiermonnikoog, Gieten, Veldhoven, Montferland and Wassenaar, the Netherlands as previously described [55]. Collected ticks were immersed in 70% alcohol and stored at -20°C until the DNA extraction. DNA from questing nymphs was extracted by alkaline lysis as previously described [56]. Detection of *R. helvetica* was done by qPCR of gltA gene using using Rick_HelvgltA_F2: ATGATCCGTTTAGGTTAATAGGCTTCGGTC and Rick_HelvgltA_R2: TTGTAAGAGCGGATTGTTTTCTAGCTGTC as forward and reverse primer as described [57].

rickA : PCR assays targeting a ~600 nt fragment of the rickA gene was performed on qPCR positive samples, as previously described [58]. In all PCR assays, DNA-free water was used as negative control. Primers used: RIC1200_F2 GGCAAAATGTTAAAAATGTTT and RIC+430_R3 CCRGYTTTTTAACCGTAGTAG. Sequences representing the complete rickA gene were extracted from newly obtained *R. helvetica* genomes, and aligned with the PCR products using the ClustalW algorithm implemented in Geneious Prime (v2023.1.1).

***DNA isolation and genome sequencing***

DNA extraction and sequencing was performed at Future Genomics Technologies BV (Leiden, The Netherlands). Ticks were ground to a fine powder using a pestle and mortar with liquid nitrogen. To extract high molecular weight DNA, a Genomic-tip 20/G kit (Qiagen Benelux BV, Venlo, The Netherlands) was used according to the standard protocol. DNA quality was measured via electrophoresis in Genomic DNA ScreenTape on an Agilent 4200 TapeStation System (Agilent Technologies Netherlands BV, Amstelveen, The Netherlands) and total DNA measured using a Qubit 3.0 Fluorometer (Life Technologies Europe BV, Bleiswijk, The Netherlands).

One microgram of the DNA samples was used to prepare a 1D ligation library using the Ligation Sequencing Kit (SQK-LSK110) according to the manufacturer's instructions (Oxford Nanopore Technologies, Oxford, United Kingdom). Oxford Nanopore Technologies (ONT) libraries were first tested on a MinION flowcell (FLO-MIN106) and subsequently run on a PromethION flowcell (FLO-PRO002) using the following settings: basecall model: high-accuracy; basecaller version: Guppy 5.0.17. Parallel aliquots of the DNA samples used for ONT sequencing were used to prepare Illumina libraries using the Nextera DNA Flex Library Prep Kit according to the manufacturers' instructions (Illumina Inc., San Diego, CA, USA). Library quality was measured via electrophoresis in D1000 ScreenTape on an Agilent 4200 TapeStation System (Agilent Technologies Netherlands BV, Amstelveen, The Netherlands). The genomic paired-end (PE) libraries were sequenced with a read length of 2 x 150 nt using the Illumina NovaSeq 6000 system.

***Data FAIRification***

The FAIR Data station [59] was used to register and submit the raw data and metadata associated with this study. The ENA "host-associated" checklist (ERC000013) was selected to meet the minimum metadata requirements for describing the biological samples and included other relevant metadata fields.

### 2.2 *R. helvetica* from cell cultures

For the cell culture, questing *I. ricinus* adult ticks were collected in August 2018 by blanket dragging in "Duin & Kruidberg", the Netherlands (52°26'05.3"N 4°37'33.0"E) and morphologically identified to species level using an identification key [53]. Samples were kept at -80°C until processing. The *R. helvetica* strain denoted as DK2, was isolated and cultured in VERO cells from an adult male *I. ricinus* tick as described in [60] and harvested as described in [61] with two modifications: here the needle and syringe protocol was implemented using 26 gauge needles and a 0.45µm syringe-driven membrane filter. For short Illumina reads, the bacterial pellet was shipped to Baseclear (Leiden, the Netherlands) and short reads were generated on the Illumina NovaSeq 6000 system (Illumina, San Diego, CA, USA) from genomic DNA extracted using the ZymoBIOMICS™ 96 MagBead DNA Kit (Zymo Research, Orange, CA). Long reads were generated at the RIVM (Bilthoven, the Netherlands) on a Nanopore GridION sequencer, DNA was extracted using the DNeasy Blood & Tissue Kit (Qiagen, Hilden, Germany), following the manufacturer's instructions.

### 2.3 Genome assembly and annotation

***Raw Data Processing***

The raw data underwent processing via a standardized workflow for Hybrid Metagenomics Assembly [62] which is registered at the WorkflowHub [63]. Workflows are written in the Common Workflow Language [64] and executed using cwltool (RRID:SCR_015528) [65]. This workflow encompasses multiple stages (Figure 1) that systematically process the raw data towards assembly. Subsequently, a semi-manual polishing procedure was employed.

llumina and nanopore reads were inspected for quality using FastQC v0.12.1 [66]. Illumina reads were filtered with fastp v0.23.2 [67] with parameters –correction, –dedup, –disable_trim_poly_g –length_required 50, –qualified_quality_phred 20, –unqualified_percent_limit 20. Possible Illumina spike in PhiX genomic reads contamination was filtered with BBMap/bbduk v38.95 [68] -k 31, reference (NC_001422.1). To filter illumina reads for selected species BBMap v38.95 [68] was used with default settings and bloom=t. Nanopore reads were filtering using minimap2 v2.24 [69] default setting, –x and map-ont. Mapped reads were kept. Reference genomes of at the time available *Rickettsia* genomes were used. The reference for *Midichloria mitochondrii* read filtering was the reference genome (CP002130.1). To filter mitochondria reads, the at the time available *Ixodes* mitochondrial genomes were used. Genome sequences were extracted from the European Nucleotide Archive. Lists of genome accessions for filtering can be found in Supplementary File 1.

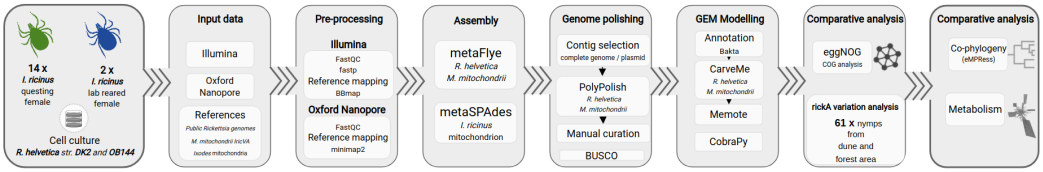


**Figure 1. Ixodes ricinus endosymbiont genome assembly and analysis.** A standardized workflow for hybrid metagenomics assembly was used (see Methods section for details). Two sources of genomic DNA were used as input; *I. ricinus* metagenomic DNA obtained from adult female ticks and *R. helvetica* genomic DNA isolated from infected Vero cell lines.

#### *Taxonomic classification of the Illumina reads*

Illumina paired end reads were filtered with fastp v0.2.23 with parameters –correction, –disable_trim_poly_g, –length_required 5, –qualified_quality_phred 20, –unqualified_percent_limit 20. For high precision taxonomic classification of the Illumina reads, the filtered reads were run through Kraken2 v2.1.2 [70] in paired end mode (`-paired-end`) with a confidence threshold (`-confidence`) of 0.5. For the Kraken2 index, the full NCBI nucleotide (nt) database downloaded from https://benlangmead.github.io/aws-indexes/k2 (date 2023-05-02) was used and was built using default kmer-length, minimizer length and minimizer spacing, 35,31,7 respectively. For species abundance estimation, Bracken v2.8 [71] was used with the previously described NCBI nt Kraken2 database with a read length (`-r`) of 150 and a threshold (`-t`) of 1000 reads and level (`-l`) 'S' for species. Eukaryotic species were filtered from the Bracken output files with the `filter_bracken_out.py` script from KrakenTools v1.2e ' [72]. To get read counts below 1000 for the resulting species, Bracken was again run on Kraken2 reports with the same parameters except with a threshold (`-t`) of 10 reads. fastANI v1.34 [70] was used for calculating average nucleotide identity (ANI). This was performed for *M. mitochondrii* and *R. helvetica* assemblies from this study and the reference genomes retrieved from the GenBank.

#### *Genome assemblies*

Regarding assembly for both the *Rickettsia helvetica* and *Midichloria mitochondrii* genomes, Flye v2.9 [73] –meta –nano-raw was used to assembly the filtered reads. Assembly polishing was performed with PolyPolish [74] v.0.5.0 in combination with bwa v0.7.17-r1188 [75]. Multiple rounds of the polishing procedure was done until no further improvement was observed regarding BUSCO score. The BUSCO score was calculated using BUSCO v5.4.4_cv1 [76] –mode geno and –lineage rickettsiales_odb10. Mitochondrial genomes were assembled using SPAdes v3.15.4 [77] -meta. Manual curation was performed afterwards by mapping the filtered reads back to its assembly.

#### *Genome annotation of Rickettsia helvetica and Midichloria mitochondrii*

The filtered Illumina and nanopore reads of all samples were mapped against the polished genome sequences to allow visualisation of the mapping files in Tablet [78]. Mitochondrial genome assemblies and the assemblies of *R. helvetica* and *M. mitochondrii* were manually circularised and the residue numbering was changed using Geneious Prime (v2023.1.1). Structural and functional annotation of the *R. helvetica* strains and the *M. mitochondrii* assemblies was done with Bakta v1.8.1 [79] with the database v5.0-full, –compliant –locus_tag and it's replicons defined. Furthermore, eggNOG-Mapper (v2.1) [80] with database v5.0 and parameters; -m diamond, –evalue 0.001 –score 60 –pident 40 –query_cover 20 –subject_cover 20 –tax_scope auto –target_orthologs all –go_evidence non-electronic –pfam_realign none, was used for the functional annotation and to determine the Clusters of Orthologous Groups (COG) for protein encoding regions. The mitochondrial genome assemblies were annotated using annotate with BLAST option implemented in Geneious Prime.

## 2.4 Phylogenetic analysis of *Ixodes ricinus* mitogenomic data

For the phylogenetic analyses, we utilized complete mitochondrial genome sequences from 18 Dutch I. ricinus genomes. To align mitochondrial data ClustalW alignments were computed using Geneious 11.1.4 software [81]. Phylogeny was inferred by IQTREE 2.1.3 [82], and the best-fit evolution model was selected based on the Bayesian information criterion (BIC) computed by implemented ModelFinder [83]. Branch supports were assessed by the ultrafast bootstrap (UFBoot) approximation [84] and the Shimodaira–Hasegawa like approximate likelihood ratio test (SH-aLRT) [85]. Tree was rooted at the midpoint. No out-group was included, because our investigation was focused on genetic similarities/differences, rather than evolutionary research questions. Tree was visualized and edited in FigTree (v1.4.1) and Inkscape (v 0.91) [86].

## 2.5 Cophylogenetic analysis

The single-copy core genes of 11 *R. helvetica* and 12 *M. mitochondrii* genomes were identified in Anvi'o 7 and made up of 1484 and 1127 single-copy gene (SCG) clusters, respectively. Gene alignments from SCG were extracted and concatenated using the program anvi-get-sequences-for-gene-clusters, with parameters: –concatenate-gene-cluster; –report-DNA-sequences. Maximum likelihood phylogenetic trees were constructed in IQ-TREE v2.2.0 [87]. The best model according to the Bayesian Information Criterion (BIC) was selected with Model Finder [88] as implemented in IQ-TREE. All models were run with Ultrafast Bootstrapping [89]. Subsequently, the eMPRess software which is a program for phylogenetic tree reconciliation under the duplication-transfer-loss (DTL) model, was used to determine whether the mitochondrial genome of *I. ricinus* and *I. ricinus* symbionts: *M. mitochondrii* and *R. helvetica* coevolved by comparing their phylogenetic relationships. The input trees were based on the results of phylogenetic analyses. The analysis was conducted using the default eMPRess parameters.

## 2.6 Genome-Scale Metabolic Model Reconstruction and Analysis

Genome-scale metabolic models (GEMs) for *M. mitochondrii* and *R. helvetica* were developed using CarveMe (v1.5.1) [90], starting with their annotated genome sequences (Ir_d9Mm and Ir_d9Rh). This process involved extracting gene annotations from the genomes and employing these to establish Gene-Protein-Reaction (GPR) rules, which link genes, proteins, and metabolic reactions. CarveMe then reconstructed the metabolic network by identifying and connecting metabolic reactions based on these annotations. For Reaction Essentiality Analysis, we performed gene or reaction deletion analysis using flux balance analysis (FBA). This method predicts flux distributions in a metabolic network by solving a linear optimization problem, where a non-zero biomass production indicates an essential reaction (see Supplementary File 2 for more details). In Determining Minimal Nutrient Requirements, an optimization problem was solved to find essential nutrients for biomass production. This involved setting up constraints like mass balance, reaction flux bounds, biomass production threshold, and nutrient uptake bounds in the optimiza-

**Table 1. Origin and deep sequencing of adult *Ixodes ricinus* ticks**

| Name | ONT (Gb) | Illumina (Gb) | Description | Collection Date | Location (habitat type) |
|---|---|---|---|---|---|
| Ir_d1 | 65.7 | 157.0 | Questing adult female | 14.10.2021 | 52.3037; 4.5331 Coastal dune |
| Ir_d2 | 19.4 | 172.4 | | | |
| Ir_d3 | 16.4 | 91.4 | | | |
| Ir_d4 | 14.4 | 156.2 | | | |
| Ir_d5 | 14.9 | 115.8 | | | |
| Ir_d6 | 32.9 | 192.0 | | | |
| Ir_d7 | 48.3 | 169.9 | | | |
| Ir_d9 | 38.4 | 158.5 | | | |
| Ir_f1 | 144.1 | 137.7 | Questing adult female | 23.03.2022 | 51.9769; 5.6992 Planted forest |
| Ir_f3 | 88.4 | 105.5 | | | |
| Ir_f6 | 69.7 | 111.3 | | | |
| Ir_f11 | 63.7 | 140.6 | | | |
| Ir_f12 | 39.0 | 120.0 | | | |
| Ir_f16 | 67.1 | 139.1 | | | |
| F1 | 53.0 | 129.8 | Questing nymph Lab-reared to female | 09.01.2020 | 51.5839; 5.4159 Planted forest |
| F2 | 94.8 | 104.8 | | | |
| DK2 | 1.22 | 0.63 | R. helvetica culture from questing male | 14.08.2018 | 52.4347; 4.6258 Coastal Dune |
| OB144/2013 | 8.71 | 4.55 | R. helvetica culture from questing nymph | 02.07.2013 | 48.3177; 12.5390 Planted forest |

tion model (Supplementary File 2). MEMOTE (v0.13.0) [91] was used to assess the quality of the GEMs. The COBRApy (v0.26.3) [92] employing Python (v3.11.3), was used for modelling simulation and analysis of each GEM using the IBM CPLEX Solver. Scripts used to reproduce the model simulations are provided on GitLab (https://git.wur.nl/unlock/projects/ticks).

### 2.7 Immunofluorescence localization studies of *R. helvetica* in ticks

Fifteen *I. ricinus* questing female ticks collected in the Amsterdamse Waterleidingduinen, the Netherlands (52°32'79.9"N, 4°54'38.6"E) on the 14.10.21 were morphologically identified to species level using an identification key [53]. All ticks were kept alive until further processing. Ticks were dissected, and gut, malpighian tubules, salivary glands, reproductive system and synganglion were collected. In addition, the same was performed on 10 ticks from a laboratory colony (BIPAR, France) to be used as controls. All tick carcasses were kept and screened for the presence of *R. helvetica* DNA by qPCR.

Organs were fixated in 4% paraformaldehyde (PFA) in PBS for 2h and then replaced by 70% ethanol and stored at -20C until used. The organs were washed by 0.5% Triton X-100 in PBS (PBST) five times, then replaced by 5% normal goat serum (Sigma) in PBST and incubated for 1h in room temperature. Afterwards, the serum was replaced by *R. conorii* commercial antibody 1:30 in PBST and incubated at 4C for 2 days. Samples were incubated with DAPI before mounting in Prolong Antifade Diamond Mountant (Life Technologies) and images were obtained using a z-stack tool in Leica DMI8 confocal microscopy. Assembled z-stacks were adjusted in Adobe Photoshop version 24.0.1 (Adobe Inc.).

### 2.8 Statistical analysis

Haplotype diversity (Hd), variance of Hd, nucleotide diversity ($\pi$), variable (polymorphic) sites, and parsimony informative sites were calculated for mitochondrial genomes of *I. ricinus* using the DNA SP6 (v6.12.03) [93].

To test whether the composition of repeats differs per prevalence and per area type (dune vs forest), we performed PERMANOVA based on Bray-Curtis dissimilarity matrix using adonis2 function from the vegan package [94].

## Results

### 3.1 Origin of genomes generated in this study

To deepen our knowledge of genome variation and transmission dynamics of *M. mitochondrii* and *R. helvetica* within *I. ricinus* ticks, our goal was to obtain the complete genomes directly from the host. For this, fourteen adult female ticks were collected, with eight originating from a coastal sand dune area (d) and six from a forested area (Table 1). Additionally, two female nymphs (F1 and F2) obtained from a forested area were moulted under laboratory conditions and added to the pool.

Furthermore, we obtained the complete genomes of two strains of *R. helvetica* using standard procedures, employing a Vero cell line as the host cell for replication. Strain DK2 was obtained from an adult male biospecimen (Table 1) while strain OB144/2013, was obtained from a nymph.

### 3.2 Deep sequencing of *I. ricinus* adult females reveals the presence and diversity of symbiotic bacteria

Each individual tick was sequenced, utilising both Illumina and ONT (Oxford Nanopore Technologies) methodologies. Using Illumina 150 x 150 nt paired-end reads as input and the NT database [95] as a reference, we applied a Kraken2-Bracken [70, 71] workflow (Figure 1) to estimate for each tick, the abundances and taxonomic classifications of the microbiome-related reads obtained. In total, more than 90% of the read-pairs that were attributed to the bacterial domain could be classified at the species level. When we applied a conservative threshold of at least 1000 read-pairs per species, Kraken2 could assign reads to 54 distinct bacterial "species" present in at least one of the sixteen ticks (Supplementary File 1). The top 3 results are summarised in Figure 2.

A significant number of paired-end reads (with a cumulative score of $> 20.000$ read pairs) were assigned to known tick borne pathogens: *Anaplasma phagocytophilum* was found to be present in tick Ir_d1 and Ir_d9, both collected from the dune area; *Borrelia afzelii* was found to be present in tick Ir_d9 and *Neoehrlichia mikurensis* [96] was present in tick Ir_f3 collected from the forested area. *Rickettsiella* species have been identified as facultative endosymbionts of *I. ricinus* ticks [97] and with more than 1 million read pairs assigned, *Ricketssiella* species appear to be present in Ir_d1, Ir_d6 and Ir_d7 (Figure 2).

Of the 14 adult *I. ricinus* females collected in the field (Table 1), eight tested positive for the presence of R. helvetica DNA by qPCR analysis (Supplementary File 1). Kraken2 analysis using the complete NT- database as reference however, suggested that *Rickettsia asiatica*, *R. conorii*, and *R. helvetica*, three species that share almost identical DNA sequences, appeared to exhibit a significant concurrent presence in these ticks. We used fastANI [98] to gain more insight into their evolutionary distances. For prokaryotes a commonly used operational definition is that if two genome sequences share over 95% average nucleotide identity (ANI), they belong to the same species. The reference strains of *R. helvetica* and *R. asiatica* show >98.66% ANI and thus are extremely closely related. When comparing the *R. helvetica* and *R. conorii* strain and the *R. asiatica* and *R. conorii* strain, the ANI values are 93.4% and 93.3% respectively. Although these high identity scores offer an explanation for the Kraken results, it's important to note that FastANI also revealed significant intragenomic rearrangements between them (Figure 3), which could potentially impact their pathogenicity.

### 3.3 Reconstruction and phylogenetic analysis of the *I. ricinus* mitochondrial genome

MT genome sizes ranged from 14562 to 14575 bp. For all, a circular genome was obtained coding for 13 protein encoding genes, 22 transfer RNA genes (tRNAs) and 2 ribosomal RNA genes (rRNAs) (Supplementary File 1). The AT content of the MT genomes ranged from 79.2% to 79.3%, a characteristic feature shared with other hard tick species [99].

A multiple alignment of the 16 mitochondrial genome sequences indicated 214 variable positions of which 147 were informative parsimony sites (excluding indels) and a mean nucleotide diversity of

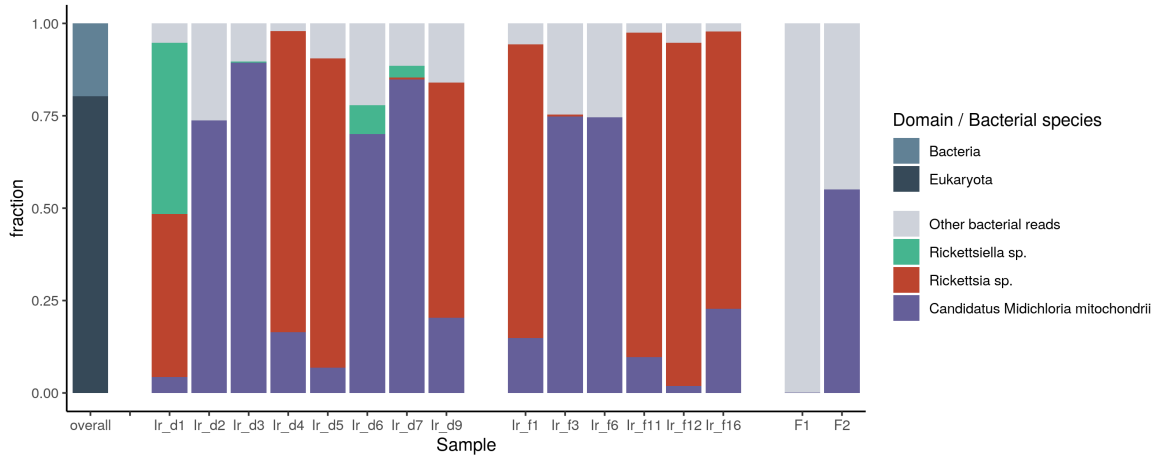


**Figure 2. Bracken distribution of classified Illumina paired-end reads at the species level**. Default parameters for kmer length (35), minimizer length (31), and minimizer spacing (7), were used in this analysis. Left: top level classification, right: classification of the bacterial domain at species level. The top 3 most prevalent species are indicated. The full analysis is available in Supplementary File 1.

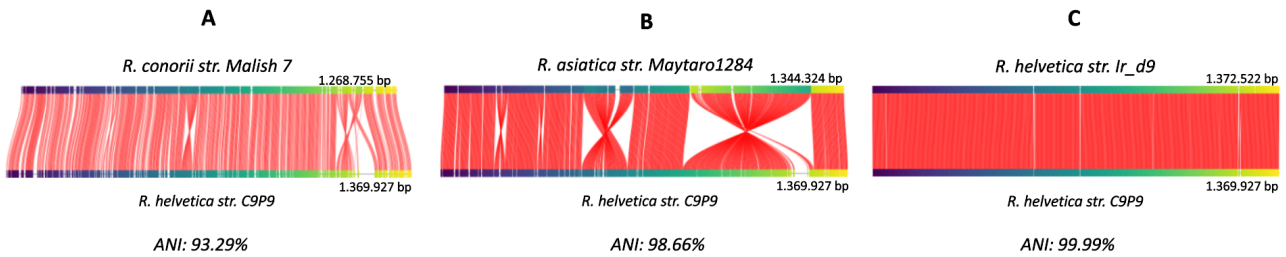


**Figure 3. Major intragenomic rearrangements between *Rickettsia helvetica* and *Rickettsia asiatica***. FastANI orthologous mappings was done using a 3kb fragment size. Red line segments denote the orthologous mappings between these fragments. Panel **A**: ANI computed between *R. conorii* strain (NC_003103.1) as query and *R. helvetica* strain C9P9 (NZ_CM001467.1) as reference. **B**: ANI computed between *R. asiatica* strain (NZ_AP019563) as query and *R. helvetica* strain C9P9 as reference. **C**: ANI computed between the *de novo* assembled *Rickettsia* strain from tick Ir_dr9 as query and *R. helvetica* strain C9P9 as reference.

0.00460. These variable sites defined a total of 15 haplotypes (mean haplotype diversity, Hd = 0.9917, with samples Ir_f1 and Ir_f3 carrying the same haplotype. The phylogenetic analysis of the mitogenomic data suggests that a locality-dependent structure based on geographic location (dune and forest) is absent (supplementary figure 2).

### 3.4 *Genome reconstruction of M. mitochondrii endosymbiotic strains*

Kraken2 analysis (Figure 2) revealed that 15 of the 16 ticks are positive for *M. mitochondria*. The exception was tick F1, initially obtained as a nymph and subsequently raised in a laboratory setting. High quality MAGs of *M. mitochondrii* could be assembled from 11 ticks (Supplementary File 1). The *de novo* assemblies shared over 99% ANI (supplementary file 2) with the *M. mitochondrii* reference strain [100] and were characterised by high a BUSCO score (> 92.9%). Genome sizes ranged from 1.190.312 to 1.191.611 bp with the exception of the assembly obtained from tick Ir_d2 which was 1.268.036 bp due to a duplication event (supplementary file 2). The average guanine cytosine (GC) content was 36.6%. All *M. mitochondrii* genomes contained 3 rRNAs, between 35-39 tRNAs, and the number of protein encoding genes varied from 1322 to 1448. EggNOG analysis suggest that the newly sequenced genomes encode a (near) complete Folate biosynthetic pathway (6 of the 7 required genes detected) and a likely complete Biotin biosynthetic pathway (all required gene detected). A complete eggNOG based functional analysis of each *M. mitochondrii* assembly is provided in Supplementary File 1.

#### *Pangenome comparison of Midichloria mitochondrii genome assemblies*

Between them, the eleven *de novo* Midichloria genome assemblies showed a significant level of genomic colinearity. In comparison with the reference strain however, many genome rearrangements were observed (supplementary file 2). Genome variant calling revealed strain variations. The total number of variants ranged from 604 to 964 (8509 total). Of these, 5029 single nucleotide polymorphisms (SNPs), 2246 insertions, 1989 deletions, and 335 complex variants were detected (Table 2).

### 3.5 Genome reconstruction of *R. helvetica* endosymbiotic strains

Of the 14 adult *I. ricinus* females collected in the field (Table 1), eight tested positive for the presence of *Rickettsia* strains by both qPCR and Kraken2 analysis and we were able to obtain the respective genomes and associated plasmids for all of them. Additionally, two genomes (DK2 and OB144) were obtained from Vero cell lines.

All ten *de novo* assemblies were characterised by a high BUSCO score (>98.9%). Genome sizes varied from 1.372.202 bp to 1.372.575 bp which is about 2,2 - 2.5 kb larger than than the C9P9 reference genome (1.369.927 bp). Consistent with the reference strain, all assemblies included a plasmid of 47184 - 48139 bp encoding 56 to 59 proteins, including 39-40 hypothetical proteins. All *R. helvetica* genomes contained 3 rRNAs, 33 tRNAs, the number of protein encoding genes ranged from 1630 to 1664 per assembly including a complete set of genes for *de novo* folate biosynthesis (Supplementary File 1).

**Table 2. Genetic variation for 11 genomes of *Midichloria mitochondrii* and 8 genomes of *Rickettsia helvetica* obtained in this study.**

| | Strain | Complex* | Deletions | Insertions | SNPs | Variant Total** | Genome Size | % Difference |
|---|---|---|---|---|---|---|---|---|
| *Midichloria mitochondrii* | F2 | 25 | 170 | 92 | 317 | 604 | 1 190 761 | 0.0059 |
| | Ir_d2 | 29 | 186 | 112 | 606 | 934 | 1 268 036 | 0.0664 |
| | Ir_d3 | 38 | 186 | 117 | 570 | 911 | 1 191 611 | 0.0066 |
| | Ir_d4 | 35 | 187 | 112 | 625 | 962 | 1 190 364 | 0.0055 |
| | Ir_d7 | 30 | 183 | 102 | 362 | 680 | 1 190 694 | 0.0058 |
| | Ir_d9 | 36 | 185 | 98 | 368 | 687 | 1 190 746 | 0.0058 |
| | Ir_f1 | 26 | 173 | 95 | 340 | 635 | 1 190 725 | 0.0058 |
| | Ir_f3 | 22 | 170 | 92 | 317 | 601 | 1 190 732 | 0.0058 |
| | Ir_f6 | 33 | 181 | 110 | 559 | 883 | 1 190 835 | 0.0059 |
| | Ir_f11 | 28 | 177 | 100 | 343 | 648 | 1 190 674 | 0.0058 |
| | Irf_16 | 33 | 191 | 116 | 622 | 964 | 1 190 312 | 0.0055 |
| *Rickettsia helvetica* | Ir_d1 | 3 | 2 | 43 | 17 | 65 | 1 372 533 | 0.0018 |
| | Ir_d4 | 2 | 2 | 43 | 15 | 63 | 1 372 384 | 0.0017 |
| | Ir_d5 | 2 | 2 | 41 | 19 | 64 | 1 372 519 | 0.0018 |
| | Ir_d9 | 3 | 2 | 43 | 18 | 66 | 1 372 522 | 0.0018 |
| | Ir_f1 | 2 | 3 | 44 | 21 | 71 | 1 372 458 | 0.0018 |
| | Ir_f11 | 2 | 2 | 43 | 13 | 60 | 1 372 442 | 0.0018 |
| | Ir_f12 | 2 | 2 | 43 | 21 | 69 | 1 372 202 | 0.0016 |
| | Ir_f16 | 2 | 4 | 44 | 31 | 82 | 1 372 575 | 0.0019 |

**Complex: the number of multiple nucleotide polymorphisms; **Variant total: the total amount of variants between the newly obtained and reference genome.*

***Comparison of R. helvetica genome assemblies***

Genome variant calling among the eight *I. ricinus* derived genome assemblies revealed a total number of variants ranging from 63 to 82 (540 in total). Of these, 155 single nucleotide polymorphisms (SNPs), 344 insertions, 19 deletions, and 18 complex variants were detected (Table 2).

Overall the novel *Rickettsia* (meta)genome assemblies revealed a very high level of genomic colinearity, among themselves, and with the *R. helvetica* reference strain (Figure 3 panel C) [101]. Most variation is due to gene splitting events leading to two or more open reading frames. Between the eight genome assemblies that were directed from a *I. ricinus* host we found three such gene splitting events. In contrast, we observed a notable increase of such events in the genomes of the DK2 strain and the C9P9 reference strain which were amplified by using Vero cell lines (Supplementary File 1).

Due to a gene splitting event the DK2 genome encodes a non-functional RickA protein (Supplementary File 1). The encoded protein plays a role in actin-based cell-to-cell motility and considered to be a putative virulence gene. [32, 102]. Further inspection of the new *R. helvetica* genomes revealed high genetic variability in the rickA gene due to copy number variation of a 33-nt-long repeat motif encoding 11 amino acids including 5 adjacent prolines ranging in number from 5 (Ir_d4) to 13 (OB144) (Supplementary File 1).

To gain additional insight into the genetic variability of the rickA gene within the tick population of the Netherlands, we sequenced the fragment of the *rick*A gene containing the repeat motif from 61 questing nymphs gathered from forest and dune regions. (Supplementary File 1). The results confirmed the observed copy number variation which varied from 5 to 11. No significant compositional difference was observed between dune and forest areas ($F_{1,7} = 1.2$, $p = .3772$), as well as between eight sampled locations with varying *R. helvetica* prevalence ($F_{1,7} = 0.4$, $p = .9101$).

## 3.6 Genome-scale metabolic modeling of *M. mitochondrii* and *R. helvetica* reveal metabolic dependencies

Due to their adaptation to rely on the host organism for survival *M. mitochondrii* and *R. helvetica* have reduced genomes that encode incomplete metabolic networks. The automatically generated GEM of *M. mitochondrii* (Ir_d9_Mm) is comprised of 1126 reactions, 881 metabolites, and 266 genes, while the constructed GEM of *R. helvetica* (Ir_d9_Rh) consists of 1123 reactions, 851 metabolites, and 274 genes. There were 349 transport reactions, 630 metabolic reactions, and 337 without any assigned genes for the model Ir_d9_Mm, whereas Ir_d9_Rh contained 399 transport reactions, 581 metabolic reactions, and 353 without any gene protein reaction associations (Table 3). This also included reactions that were essential for biomass production in the GEMs. There were also genes that encoded enzyme complexes, but were not associated with reactions (36 for Ir_d9_Mm, and 49 for Ir_d9_Rh). The reason for the missing GPR association was mainly: (i) the genome annotation is incomplete or contains errors (ii) there is incomplete knowledge about specific metabolic pathways or poorly characterised genes, and (iii) different genes encode proteins with similar functions, and any of these genes can catalyse a specific reaction. Nevertheless, from MEMOTE analysis, the Ir9_Mm and Ir9_Rh GEMs received high-quality overall scores of 84% and 68% (supplementary File 3).

**Table 3.** Summary of genome-scale metabolic models of *M. mitochondrii* and *R. helvetica*

| | | Ir_d9_Mm | Ir_d9_Rh |
|---|---|---|---|
| Total No. of Reactions | | 1126 | 1123 |
| Total No. of Metabolites | | 881 | 851 |
| Total No. of Genes | | 266 | 274 |
| Reactions | Transport Reactions | 349 | 399 |
| | Metabolic Reactions | 630 | 581 |
| | Without GPR associations | 337 | 353 |
| Metabolites | Unique metabolites | 881 | 851 |
| | Medium components | 144 | 139 |
| Genes | Enzyme Complexes | 36 | 49 |

The structure of metabolic networks in genome-scale models provides valuable information about the organization, connectivity, and functional properties of the metabolic system. Network maps were generated for both GEMs of *M. mitochondrii* and *R. helvetica*, revealing the overall connectivity pattern of the metabolic reactions and their interdependencies (Figure 4A and 4B, (Supplementary File 2)). Here, we observed the flow of metabolites, the presence of branching pathways, and the overall organization of the metabolic system differed in *M. mitochondrii* and *R. helvetica*. In particular, the network topology of Ir9_Mm GEM and Ir_d9_Rh GEM differs substantially regarding amino acid and nitrogen metabolism when inspecting their size and arrangements. The network motifs of the two models also point to differences in central carbon and fatty acid metabolisms. For instance, the central carbon metabolism appears to be more tightly connected to nitrogen metabolism in Ir_d9_Rh GEM compared to Ir_d9_Mm GEM. Despite these differences in the GEM networks, Ir_d9_Rh GEM and Ir_d9_Mm GEM share

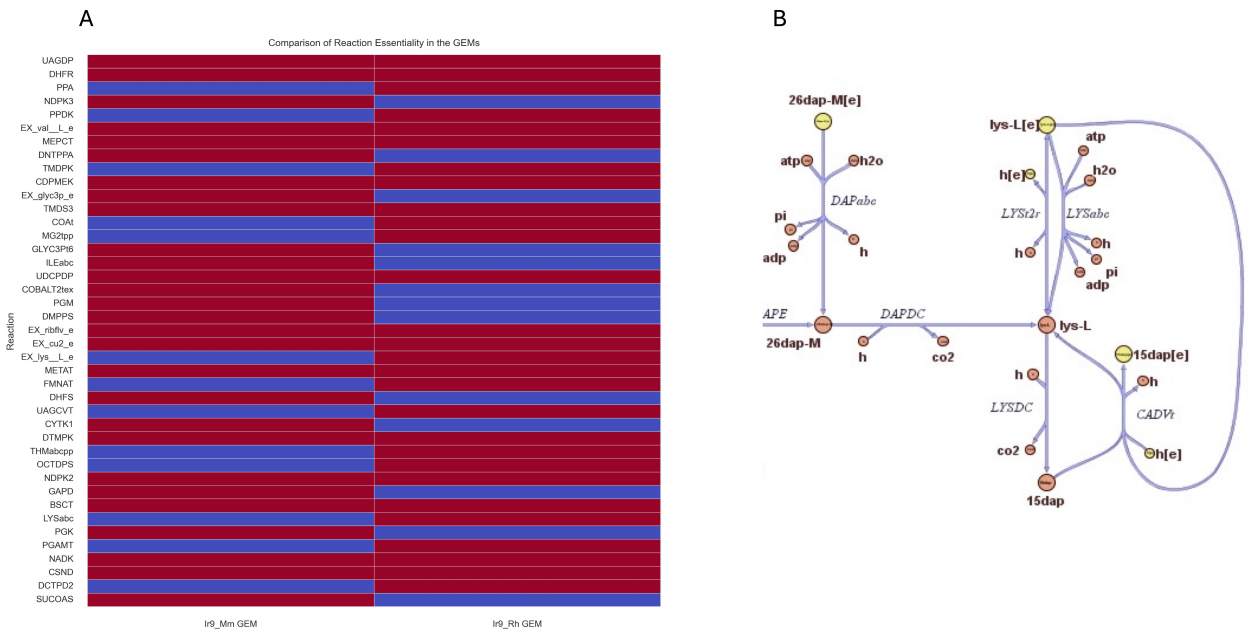


**Figure 4. Genome-scale metabolic constructions and analysis of *M. mitochondrii* and *R. helvetica*.** Heatmap comparing *M. mitochondrii* (Ir_d9_Mm GEM) and *R. helvetica* (Ir9_Rh GEM) where a subset of the essential reactions is depicted. Furthermore, blue and red panels represent which reactions are not essential or essential, respectively (panel A). Note: Complete heatmap comparing reaction essentiality of the two GEMs is contained in the supplementary material. Network map showing the network map of lysine synthesis pathway highlighting specific essential reactions in the Ir_d9_Mm GEM for *M. mitochondrii* (Ir_d9_Mm GEM) (panel B).

many similar reactions and pathways, overlapping in 802 reactions. Each GEM also contained a reasonable number of unique reactions and pathways 300 for Ir_d9_Rh GEM and 429 for Ir_d9_Mm GEM. More specifically, the Ir_d9_Mm GEM contained unique reactions and pathways related to pantothenic acid (vitamin B5) and niacin (vitamin B3). Lastly, a reaction essentiality analysis was performed indicating which reactions that need to be present to obtain growth in models. It appears that 8.70% and 8.17% of the reactions in *M. mitochondrii* and *R. helvetica*, respectively, were essential for *in silico* growth (Supplementary Model Figure 2D and 2E see (Supplementary File 3)). The reaction essentiality analysis revealed that reactions linked to lysine synthesis pathways were vital for the growth of *R. helvetica* but not for *M. mitochondrii* (see Figure 4).

### 3.7 Cophylogenetic analysis between *I. ricinus* and symbionts

To determine whether symbiont-tick pairs are co-evolved, the eMPRess phylogenetic tree alignment software following the duplication-transfer-loss model was used to compare the phylogenetic relationships of symbionts and ticks. The analysis was performed separately for two pairs: *M. mitochondrii*-*I. ricinus* and *R. helvetica*–*I. ricinus* (Figure 5). The results showed that a total of 12 events, including eight cospeciation events, two transfers, and two losses, occurred between *M. mitochondrii* and *I. ricinus*, over evolutionary time; of these events, six were robustly supported. The results of this analysis refuted the null hypothesis that the tick and *M. mitochondrii* trees and tip associations are formed due to chance at 0.01 level in host-symbiont relationships (P value = 0.0099). Therefore, we concluded that these *I. ricinus* - *M. mitochondrii* pairs have coevolved. The results for the *R. helvetica* - *I. ricinus* pair did not indicate the rejection of the coevolution hypothesis (P- value = 0.77).

### 3.8 *Rickettsia helvetica* localization in adult female ticks

The localization of *R. helvetica* in adult *I. ricinus* females was investigated in order to explore the nature and homogeneity of its distribution in tick tissues and potential transmission routes. *Rickettsia helvetica* was successfully visualised using laser microscopy in 5 out of the 15 adult females treated (Figure 6). The same ticks were also qPCR positive for *R. helvetica*. All controls were negative (Supplementary File 1). *Rickettsia helvetica* could be clearly visualised in salivary glands, malpighian tubules, in the gut and in reproductive organs (Figure 7, Supplementary figure 5). The distribution of *R. helvetica* in tick organs varied between specimens (Supplementary File 1). In the reproductive system, *R. helvetica* could be visualised both in the female oviduct (2 ticks, Figure 6C,D) and in the *receptaculum seminis* (RS) (3 ticks, Figure 6 A,B) which serves as the storage site for sperm introduced during copulation.

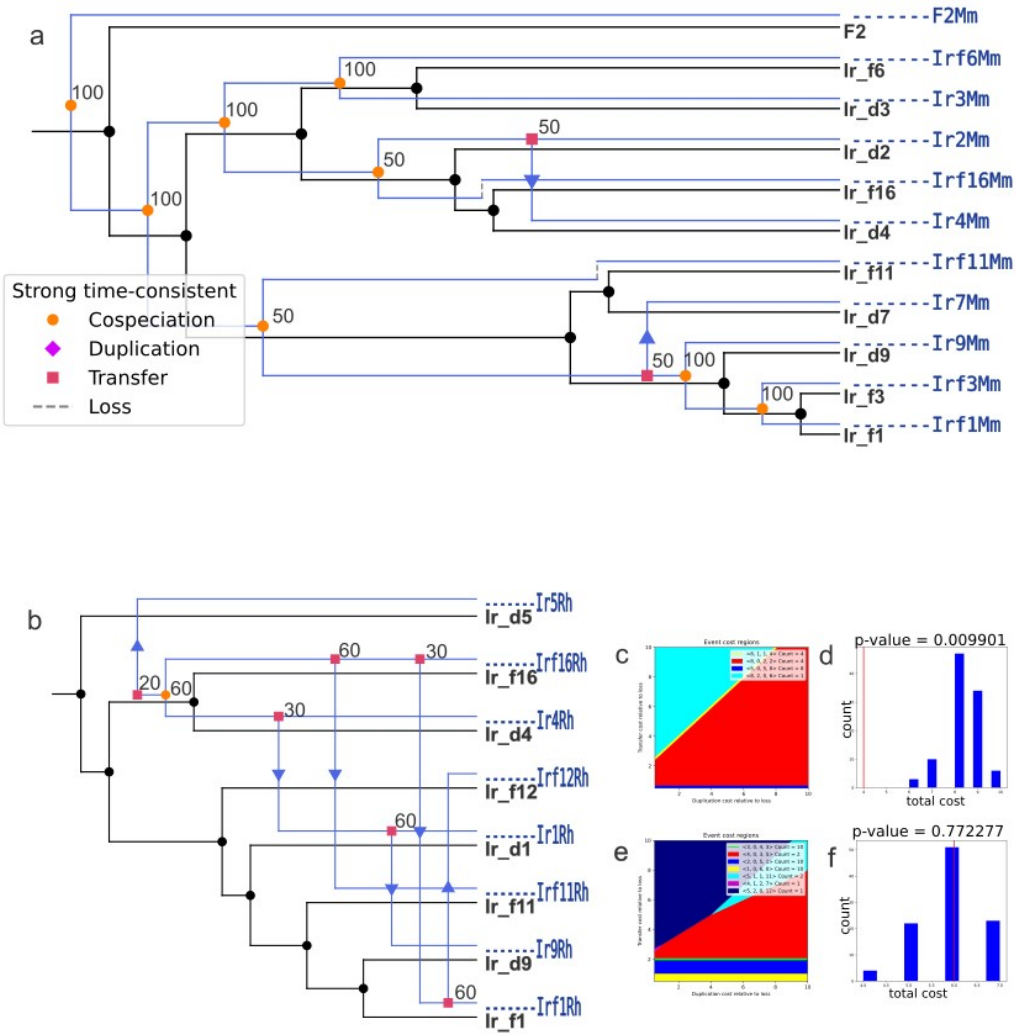


**Figure 5. Cophylogenetic analysis between *I. ricinus* ticks and its symbionts**. a) Phylogenetic reconciliation of *I. ricinus* (displayed in black) and *M. mitochondrii* (in blue). b) Phylogenetic reconciliation of *I. ricinus* (displayed in black) and *R. helvetica* (in blue); c); d) P-value histogram of host and *M. mitochondrii*; e); f) P-value histogram of host and *R. helvetica*; the optimal reconciliation cost of the coevolution trees is indicated with a red line, and the optimal cost of the same trees constructed with tip associations permuted at random is shown in blue columns.

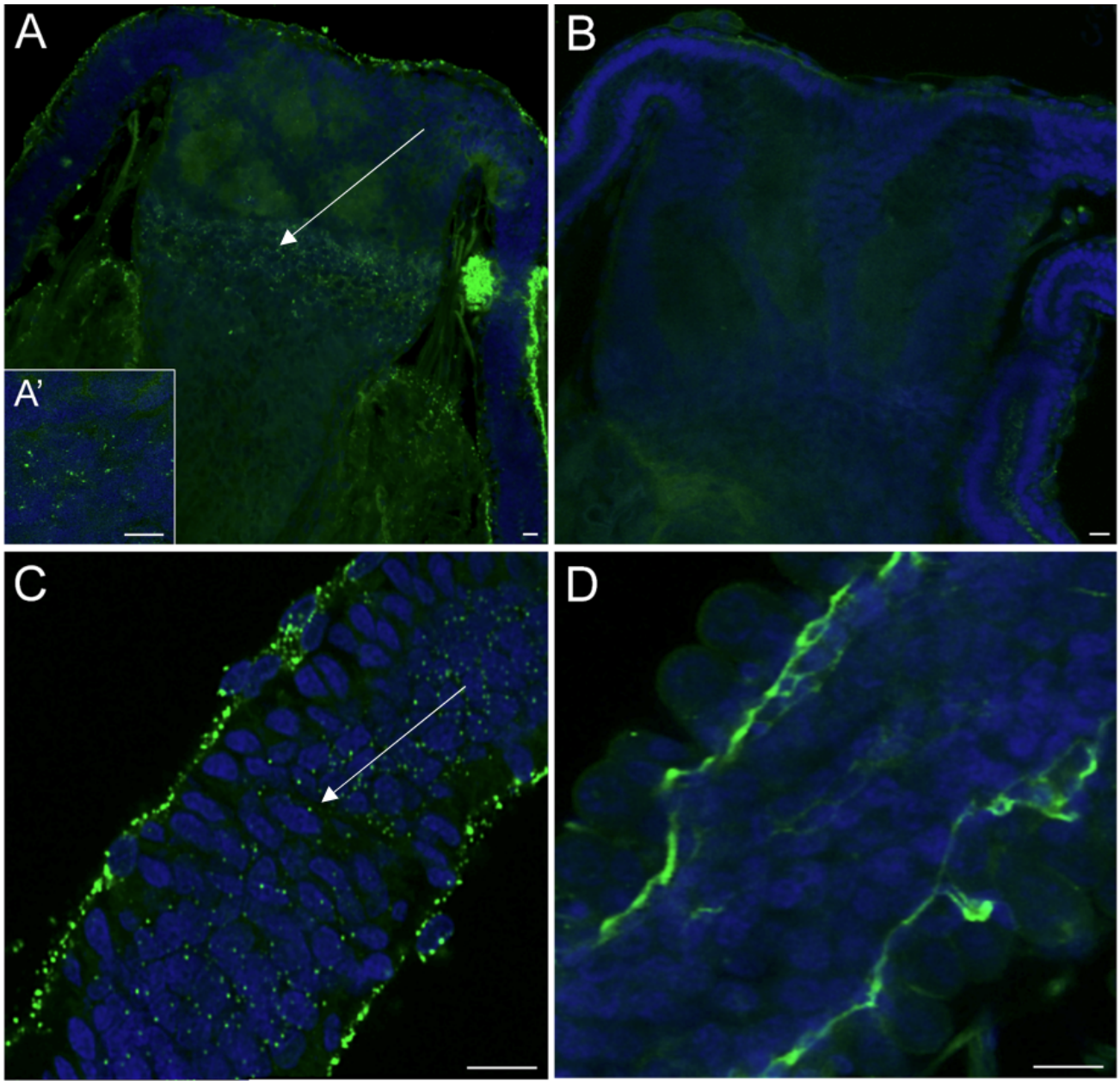


**Figure 6. Localization of *Rickettsia helvetica* in adult females.**, Blue: DAPI, Green dots: *Rickettsia* specific binding. A) R. helvetica positive *receptaculum seminis* X40 A') *R. helvetica* positive *receptaculum seminis* X100, B) Control *receptaculum seminis* , C) *R. helvetica* positive oviduct X40, D) Control oviduct. Note that tissue specific autofluorescence can be observed in the treatment and control groups. Scale-bar: 10$\mu$m

## 4. Discussion

### 4.1 Endosymbiont genome sequencing

Sequencing of bacterial genomes has greatly enhanced our understanding of the biology of numerous bacterial pathogens. Conducting whole-genome sequencing of obligate intracellular bacteria often involves essential time and resource consuming steps [46]. These steps include isolating the microorganism from the host, infecting an intermediate replication host with the associated risk of host adaptation, and purifying the microbial DNA from this host. To address these challenges, we employed a direct deep-sequencing method to acquire genomes of *M. mitochondrii* and *R. helvetica*, aiming to investigate their transmission dynamics and lifestyle.

The *I. ricinus* holobiome is is still being discovered. The draft of the host genome has been only recently been assembled [103] and the microbial component is underexplored. We used the Kraken2 tool to profile of what is present in the bacterial domain using the NT database comprising of (partially) non-redundant nucleotide sequences from all traditional public databases except for the WGS draft genome assembly database as a reference. The Kraken2 tool employs exact-match database queries of k-mers to classify sequences within a dataset down to species level. At this level Kraken2 was able to assign across the 16 individual female ticks 54 "species" each with a paired-end read count of 1000 or more.

This number corresponds with results from the analysis of the complete microbiome of 106 female *I. ricinus* ticks using 16S rRNA gene amplicon sequencing, with a reported mean alpha-diversity of 32.8 [104]. At genus level these samples were dominated by *Candidatus Midichloria*, which were observed to be present in 99.5% of the tick samples, followed by *Pseudomonas, Methylobacterium, Sphingomonas,* and *Rickettsia*. *Rickettsiella*, a facultative endosymbiont of *I. ricinus* ticks [97], was present in 60.9% of these tick samples. The microbiomes of our biospecimens exhibited a dominant presence of *M. mitochondrii* which was present in 15 out of 16 biospecimens. *Rickettsia helvetica* was abundant in eight biospecimens, while *Rickettsiella* species were abundantly present in three of these biospecimens. Furthermore, we did see the presence of multiple *Pseudomonas, Mycobacterium, Mycobacteroides* and *Sphingomonas* species. Note that the sensitivity of a Kraken2 search is significantly influenced by the type of genetic data is available for these species in the NT database being 16S sequences, individual gene (fragments) and complete genomes implicating that Kraken2 read-counts cannot directly be used to estimate relative species abundances.

As there is a reference genome available for *M. mitochondrii* and *R. helvetica* species, employing fixed-length Illumina read-pairs as input allowed us to directly utilize the Kraken2 output for estimating whether there exists adequate short-read genome coverage to reconstruct the complete microbial genomes of interest. In alignment with the outcomes from Kraken2, we were able to obtain eleven complete and four draft genomes of *M. mitochondrii* and, coinciding with qPCR analysis results, eight complete *R. helvetica* genomes along with their associated plasmids.

### 4.2 *Rickettsia helvetica*

The prevalence of *R. helvetica* in questing ticks has been shown to greatly differ between dune and forest areas in the Netherlands [25, 31, 105]. Although our findings point to some heterogeneity in the rickA virulence gene, there seems to be no genetic basis for the differences in prevalence of *R. helvetica* in dune versus forest areas. Thus two remaining possibilities should be further explored. Firstly, the possibility of *R. helvetica* giving ticks in dune areas an adaptive advantage in relation with local abiotic conditions has not been fully explored. The role of *R. helvetica* in this case could be related to nutrient acquisition, waste elimination, or to physical characteristics. For example, *Rickettsia* has been shown to enhance tick motility in *Dermacentor variabilis* [106]. Secondly, the possibility of interactions with other symbionts within the tick host should be explored as *R. helvetica* has been shown to modulate the microbiome of *I. ricinus* [107] and it has been found to be negatively correlated with certain symbionts such as *Spiroplasma ixodetis* and *M. mitochondrii* [31, 2]. It has been hypothesised that perhaps the biological roles of *S. ixodetis* and *R. helvetica* overlap, making their simultaneous maintenance energetically superfluous for the tick host [31], but this theory has yet to be proven. Nor has the option of other bacterial interactions been fully researched.

Our comparative analyses showed near absolute genetic homogeneity among the generated *R. helvetica* genomes (99.96-100%). %) and only a slight deviation from the published strain C9P9. In the latter case, the observed differences in chromosome size could be due to different technological platforms, assembly methods, and even geographic origins. The congruous genetic build-up among the *R. helvetica* genomes was punctuated almost exclusively by the gene encoding for the surface protein RickA. The sequence of the *rick*A gene showed high genetic variation between the genomes generated in this study as well as between genes obtained from 61 additional ticks from the Netherlands. RickA has been shown to induce actin polymerization, and hence actin-based motility, in some *Rickettsia* species [35, 108]. However, a previous study found the RickA protein in *R. helvetica* isolate AS819 to be insufficient to promote actin-based motility *in-vitro*, which spread instead through cell break-down and bacterial release [24]. The inability of the studied isolate to spread through actin-based motility was explained by a disrupted *sca*2 gene, another virulence gene believed to have a more prominent role than the *rick*A gene in the cell to cell spread of *Rickettsias* [109]. Our genomes revealed no truncated sca2 sequences, however, the rickA gene greatly differed in length due to a repeat motif. We hypothesise these repeats may affect the functionality of the rickA protein within *R. helvetica*, giving rise to variation in virulence. This observation is supported by the dose-dependent manner in which rickA induced cell motility in *R. conorii* [35]. Moreover, when expressing a heterologous rickA gene, *R. bellii* moved at higher velocities than its wild-type counterparts [110]. If the diverse rickA sequence length translates into different motility-associated phenotypes, it could explain the seemingly sporadic pathogenicity we observe for *R. helvetica*, as well as its low and inconsistent prevalence rate in wildlife hosts. This heterogeneity could also explain why two different mice models showed no substantial rickettsemia following an infection challenge with *R. helvetica* [111], and should be taken into account when exploring the infection potential of *R. helvetica* strains.

To date, no wildlife reservoir has been found for *R. helvetica*. This has led to the assumption that *I. ricinus*, which transmits *R. helvetica* transovarially [112], acts as its main reservoir in nature [25]. This close tick-symbiont interaction was not reflected in our findings which showed the absence of co-phylogeny between *R. helvetica* and the mitochondrial genomes of the *I. ricinus*. The lack of co-evolution between *I. ricinus* and *R. helvetica* may be partly due to a mixed transmission strategy encompassing vertical and horizontal routes. The presence of *R. helvetica* in the RS, as shown by our immunofluorescence findings, strongly suggests the possibility of paternal transmission for *R. helvetica* in *I. ricinus*. Paternal transmission of *Rickettsia* has been identified in the leafhopper *Nephotettix cincticeps* [113] and it has been hypothesised that a mixed mode of transmission (maternal and parental) might allow for mixing of different symbiont lineages thus allowing for the evolution of virulent variants [114]. *Rickettsias* have also been detected in the spermatids of *Dermacentor silvarum* and *I. ricinus* ticks [115, 116]. Thus, the possibility of a different genetic makeup for *Rickettsia* populations found in reproductive tick organs should be considered in future studies.

### 4.3 *Midichloria mitochondrii*

The obligate endosymbiont *M. mitochondrii* is located in the mitochondria and the cytoplasm of the oocytes of the European hard tick, *I. ricinus*. In our study, we found 15 of 16 ticks positive for *M. mitochondrii*, suggesting that this symbiont is widely distributed among a large proportion of ticks. This result is consistent with previous reports that nearly 100% of *I. ricinus* females and larvae and nearly 50% of nymphs and males were infected with this Mm [117, 118, 9, 119]. Importantly, the only tick in which no *M. mitochondrii* was detected was a nymph that had been artificially fed and molted under laboratory conditions. The genomes of *M. mitochondrii* as presented in this study are approximately 5% larger and have a different structural arrangement than the published assembly (Acc. No.: NC_015722.). The observed differences in chromosome size and structure could potentially be due to different technological platforms, assembly methods, and even geographic origins. However, we did not notice any differences connected to the tick habitat origin. The extraction of 11 M. mitochondrii genomes, each from a single tick, provides insight into the potential genomic variability of this symbiotic bacterium in its tick host. Midichloria mitochondrii exhibits a unique feature to colonize multiple compartments in a tick body, including ovaries, salivary glands [120], Malpighian tubules, tracheae and guts [121]. In this context, each genome generated in our study represents a mixture of genomes from bacteria, inhabiting different ecological niches within the tick body.. Subsequently, in the eMPRess reconciliation analysis, we showed a significant coevolutionary relationship between M. mitochondrii and its tick host, I. ricinus. This finding supports the notion of a long-standing symbiotic relationship between M. mitochondrii and I. ricinus, indicating that the vertical mode is this symbiont's main mode of transmission. Also, the observed strong cophylogeny between M. mitochondrii and its host's mitochondria is in opposition to a hypothesis that this symbiont undergoes horizontal transmission. Although M. mitochondrii has been shown to be localized in tracheae, salivary glands, and rostrum as well as it has been detected in the blood of experimentally infested rabbits, it is unlikely that it utilizes horizontal transmission to spread within the tick population under natural conditions.

### 4.4 Symbiont metabolic integration

Genome-Scale Metabolic Models (GEMs) provide a means to uncover new biological insights that go beyond what genomics can offer. A key application involves predicting the viability of an organism under specific conditions. This simulation approach has been utilized to identify potential metabolic drug targets, enabling the effective targeting of pathogens [122].

Due to their long-term relationship with the tick host, both *M. mitochondrii* and *R. helvetica* underwent genome reduction, leading to incomplete metabolic networks. The analysis suggests that *M. mitochondrii*'s *in silico* growth necessitates the inclusion of pantothenate (vitamin B5) and glycerol-3-phosphate (G3P) in the growth medium. G3P, a key metabolite in metabolic pathways such as glycolysis, gluconeogenesis, and lipid metabolism, is abundantly available in mitochondria. Its role is pivotal in the glycerol phosphate shuttle, facilitating the transfer of reducing equivalents to the mitochondrial matrix. Pantothenate is vital for energy metabolism and the synthesis of coenzyme A (CoA), a coenzyme integral to mitochondrial metabolic reactions. Our findings about the growth requirements of *M. mitochondrii* are in line with the evolutionary adaptation of this symbiont to reside in its host's mitochondria. Nevertheless, as ticks cannot synthesize pantothenate, there could be potentially other bacterial symbionts producing this vitamin to be utilized by *M. mitochondrii*.

The GEM for *R. helvetica* highlights a dependency on lysine for *in silico* growth, as demonstrated in (Figure 4B). This requirement likely results from an incomplete lysine biosynthesis pathway, a characteristic shared with *Rickettsia prowazekii* [123, 124], as previously identified. Research has consistently shown that *Rickettsia* species lack comprehensive amino acid biosynthesis pathways, particularly for essential amino acids such as lysine [125, 126]. Therefore, *R. helvetica* must obtain lysine from the blood meal ingested by its tick host or from other tick symbionts, however, the latter has not been explored.

In parallel, we investigated the supportive contribution of the *R. helvetica* and *M. mitochondrii* symbionts to their tick host related to the provision of specific nutrients. Tick genomes do not contain genes responsible for *de novo* synthesis of several essential vitamins and as they feed exclusively on vertebrate blood, which is deficient in essential micronutrients. Therefore, they are often dependent on their symbionts in periods of increased biosynthetic demands. Here, we show that *M. mitochondrii* encodes a (near) complete folate biosynthetic pathway and a likely complete biotin biosynthetic pathway, which is in line with previous findings by Olivieri et al. [127] and Buysse et al. [128].

The genome of *R. helvetica* obtained in our study includes a complete set of genes for *de novo* folate biosynthesis, which is the first report of the folate pathway in this *Rickettsia* species. Interestingly, the folB gene is replaced by PTPS-III, which has been observed in other bacteria. The genomes of other symbiotic species from spotted fever group *Rickettsia* such as *Rickettsia* species phylotype G021 of *I. pacificus* and *R. buchneri* of *I. scapularis* also contain complete pathways for folate biosynthesis. Similar to *Rickettsia* species phylotype G021 and contrary to *R. buchneri*, the genome of *R. helvetica* does not have genetic capacity to bio-synthesize biotin.

## 5. Conclusion

In this study we observed the metabolic and phylogenetic interactions of *M. mitochondrii*, a known tick symbiont, and *R. helvetica*, a symbiont of unknown pathogenicity, with *I. ricinus*. Our findings, suggesting paternal transmission of *R. helvetica*, a transmission mode relatively unexplored in ticks, require validation through experimental investigations. Moreover, the identified genetic variations in the *rickA* virulence gene of *R. helvetica* have the potential to influence its infectivity and transmission dynamics and should be further explored. This information is important for describing potential approaches to tick management and tick-borne disease control in the near future.

Although there is a growing recognition that the tick microbiota influences the transmission and spread of tick-borne pathogens, existing knowledge about the interactions among members of the *I. ricinus* microbiota and the potential coexistence of pathogens within the tick microbiota remains limited. The use of deep sequencing enables the direct extraction of complete genomes of symbionts and genetic data from host organisms, offering a robust method for gaining insights into these interactions.

### Author contributions

Conceptualization, H.S., P.J.S., J.J.K., P.M.L, T.A.; Methodology, H.S., P.J.S., P.M.L, T.A, J.J.K, L.S.; Investigation, P.M.L, T.A, J.J.K., B.N., W.T.S.J., A.I.K.; Writing – Original Draft, H.S., P.J.S., P.M.L, T.A., W.T.S.J.; Writing – Review & Editing, P.M.L, T.A, J.J.K., B.N., W.T.S.J., L.S., H.S., P.J.S., G.D., A.I.K.; Funding Acquisition, H.S. Resources, H.S., P.J.S., L.S., G.D.; Supervision, H.S., P.J.S.; All authors reviewed and approved the manuscript.

### Competing Interests

The authors declare that they have no competing interests.

## Supplementary Files

Supplementary File 1 (XLSX): Information about the strains, coverage, busco, ani and tera analysis, genome accessions, eggNOG annotation, RickA and co-linearity analysis.
Supplementary File 2 (PDF): FastANI orthologous mapping of *M. mitochondria* genomes
Supplementary File 3 (PDF): Genome-scale modelling details.
Supplementary File 4 (PDF): Phylogenetic tree of the mitochondrial *Ixodes ricinus*
Supplementary File 5 (PDF) : *Rickettsia helvetica* localization in adult female ticks
The supplementary files: https://git.wur.nl/unlock/projects/ticks/-/tree/main/supplementary_material

## Data & Code availability

The data supporting the findings of this study have been deposited in the European Nucleotide Archive (ENA). This dataset includes Oxford Nanopore Technologies (ONT) and Illumina sequencing data for multiple *Ixodes ricinus* specimens.

**Project:** PRJEB70514

**ONT:** ERR12319604, ERR12319605, ERR12319607, ERR12319608, ERR12319610, ERR12319612, ERR12319613, ERR12319614, ERR12319616, ERR12319618, ERR12319620, ERR12319623, ERR12319624, ERR12319627, ERR12319628, ERR12319631, ERR12319632, ERR12319593, ERR12319595, ERR12319597, ERR12319598, ERR12319599, ERR12319600, ERR12319602

**Illumina:** ERR12319603, ERR12319606, ERR12319609, ERR12319611, ERR12319615, ERR12319617, ERR12319619, ERR12319621, ERR12319625, ERR12319626, ERR12319629, ERR12319630, ERR12319633, ERR12319622, ERR12319594, ERR12319596, ERR12319601

**Simulation code:** The code used for the model simulations can be found at https://git.wur.nl/unlock/projects/ticks

**Genome-Scale Models:** The GEMs as well as accompanying MEMOTE[91] and FROG Analysis[129] reports can be found in a public repository on BioModels: https://www.ebi.ac.uk/biomodels/. For the *M. mitochondrii* GEM, see here: MODEL2404170001. For the *R. helvetica* GEM, see here: MODEL2404170002.

## Funding

B.N.,W.T.S.J, P.J.S, and J.J.K acknowledge the Dutch Research Council (NWO), and Wageningen University & Research for their financial contribution to the Unlock initiative (NWO: 184.035.007). T.A. and H.S. were supported by funding from the Dutch Ministry of Health, Welfare and Sport.

## References

1. Sprong H, Azagi T, Hoornstra D, Nijhof AM, Knorr S, Baarsma ME, et al. Control of Lyme borreliosis and other Ixodes ricinus-borne diseases. Parasites & vectors 2018;11:145.
2. Krawczyk AI, Röttjers S, Coimbra-Dores MJ, Heylen D, Fonville M, Takken W, et al. Tick microbial associations at the crossroad of horizontal and vertical transmission pathways. Parasites & vectors 2022 October;15(1):380.
3. Tijsse-Klasen E, Koopmans MPG, Sprong H. Tick-borne pathogen - reversed and conventional discovery of disease. Frontiers in public health 2014;2:73.
4. Azagi T, Hoornstra D, Kremer K, Hovius JWR, Sprong H. Evaluation of Disease Causality of Rare Ixodes ricinus-Borne Infections in Europe. Pathogens (Basel, Switzerland) 2020;9:150.
5. Benelli G. Pathogens Manipulating Tick Behavior-Through a Glass, Darkly. Pathogens (Basel, Switzerland) 2020;9:664.
6. Bonnet SI, Binetruy F, Hernández-Jarguín AM, Duron O. The Tick Microbiome: Why Non-pathogenic Microorganisms Matter in Tick Biology and Pathogen Transmission. Frontiers in cellular and infection microbiology 2017;7:236.
7. Lewis D. The detection of rickettsia-like microorganisms within the ovaries of female Ixodes ricinus ticks. Zeitschrift fur Parasitenkunde (Berlin, Germany) 1979;59:295–8.
8. Sacchi L, Bigliardi E, Corona S, Beninati T, Lo N, Franceschi A. A symbiont of the tick Ixodes ricinus invades and consumes mitochondria in a mode similar to that of the parasitic bacterium Bdellovibrio bacteriovorus. Tissue & cell 2004;36:43–53.
9. Sassera D, Beninati T, Bandi C, Bouman EAP, Sacchi L, Fabbi M, et al. 'Candidatus Midichloria mitochondrii', an endosymbiont of the tick Ixodes ricinus with a unique intramitochondrial lifestyle. International journal of systematic and evolutionary microbiology 2006 November;56(Pt 11):2535—2540. https://doi.org/10.1099/ijs.0.64386-0.
10. Sassera D, Lo N, Bouman EAP, Epis S, Mortarino M, Bandi C. "Candidatus Midichloria" endosymbionts bloom after the blood meal of the host, the hard tick Ixodes ricinus. Applied and environmental microbiology 2008;74:6138–40.
11. Floriano AM, Batisti Biffignandi G, Castelli M, Olivieri E, Clementi E, Comandatore F, et al. The evolution of intramitochondriality in Midichloria bacteria. Environmental microbiology 2023;25:2102–2117.
12. Olivieri E, Epis S, Castelli M, Varotto Boccazzi I, Romeo C, Desirò A, et al. Tissue tropism and metabolic pathways of Midichloria mitochondrii suggest tissue-specific functions in the symbiosis with Ixodes ricinus. Ticks and tick-borne diseases 2019;10:1070–1077.
13. Murray GGR, Weinert LA, Rhule EL, Welch JJ. The Phylogeny of Rickettsia Using Different Evolutionary Signatures: How Tree-Like is Bacterial Evolution? Systematic biology 2016;65:265–79.
14. Nilsson K, Lindquist O, Påhlson C. Association of Rickettsia helvetica with chronic perimyocarditis in sudden cardiac death. Lancet 1999 Oct;354(9185):1169–1173.
15. Fournier PE, Grunnenberger F, Jaulhac B, Gastinger G, Raoult D. Evidence of Rickettsia helvetica infection in humans, eastern France. Emerg Infect Dis 2000 Jul;6(4):389–392.
16. Fournier PE, Allombert C, Supputamongkol Y, Caruso G, Brouqui P, Raoult D. Aneruptive fever associated with antibodies to Rickettsia helvetica in Europe and Thailand. J Clin Microbiol 2004 Feb;42(2):816–818.
17. Nilsson K. Septicaemia with Rickettsia helvetica in a patient with acute febrile illness, rash and myasthenia. J Infect 2009 Jan;58(1):79–82.
18. Nilsson K, Elfving K, Pahlson C. Rickettsia helvetica in patient with meningitis, Sweden, 2006. Emerg Infect Dis 2010 Mar;16(3):490–492.
19. Nilsson K, Wallménius K, Påhlson C. Coinfection with Rickettsia helvetica and herpes simplex virus 2 in a young woman with meningoencephalitis. Case Rep Infect Dis 2011 Oct;2011:469194.
20. Koetsveld J, Tijsse-Klasen E, Herremans T, Hovius JWR, Sprong H. Serological and molecular evidence for spotted fever group Rickettsia and Borrelia burgdorferi sensu lato co-infections in The Netherlands. Ticks and tick-borne diseases 2016;7:371–7.
21. Ocias LF, Dessau RB, Lebech AM, Jørgensen CS, Petersen RF, Krogfelt KA. Evidence of rickettsiae in Danish patients tested for Lyme neuroborreliosis: a retrospective study of archival samples. BMC infectious diseases 2018;18:325.
22. Esteves T, Aparicio G, Garcia-Patos V. Is there any association between Sarcoidosis and infectious agents?: a systematic review and meta-analysis. BMC pulmonary medicine 2016;16:165.

23. Rizzoli A, Silaghi C, Obiegala A, Rudolf I, Hubálek Z, Földvári G, et al. Ixodes ricinus and Its Transmitted Pathogens in Urban and Peri-Urban Areas in Europe: New Hazards and Relevance for Public Health. Frontiers in public health 2014;2:251.
24. Speck S, Kern T, Aistleitner K, Dilcher M, Dobler G, Essbauer S. In vitro studies of Rickettsia-host cell interactions: Confocal laser scanning microscopy of Rickettsia helvetica-infected eukaryotic cell lines. PLoS neglected tropical diseases 2018 February;12(2):e0006151.
25. Sprong H, Wielinga PR, Fonville M, Reusken C, Brandenburg AH, Borgsteede F, et al. Ixodes ricinus ticks are reservoir hosts for Rickettsia helvetica and potentially carry flea-borne Rickettsia species. Parasites & vectors 2009;2:41.
26. Inokuma H, Seino N, Suzuki M, Kaji K, Takahashi H, Igota H, et al. Detection of Rickettsia helvetica DNA from peripheral blood of Sika deer (Cervus nippon yesoensis) in Japan. Journal of wildlife diseases 2008;44:164–7.
27. Boretti FS, Perreten A, Meli ML, Cattori V, Willi B, Wengi N, et al. Molecular Investigations of Rickettsia helvetica infection in dogs, foxes, humans, and Ixodes ticks. Applied and environmental microbiology 2009;75:3230–7.
28. Elfving K, Malmsten J, Dalin AM, Nilsson K. Serologic and Molecular Prevalence of Rickettsia helvetica and Anaplasma phagocytophilum in Wild Cervids and Domestic Mammals in the Central Parts of Sweden. Vector borne and zoonotic diseases (Larchmont, NY) 2015;15:529–34.
29. Hornok S, Kováts D, Csörgő T, Meli ML, Gönczi E, Hadnagy Z, et al. Birds as potential reservoirs of tick-borne pathogens: first evidence of bacteraemia with Rickettsia helvetica. Parasites & vectors 2014;7:128.
30. Michelet L, Delannoy S, Devillers E, Umhang G, Aspan A, Juremalm M, et al. High-throughput screening of tick-borne pathogens in Europe. Frontiers in cellular and infection microbiology 2014;4:103.
31. Krawczyk AI, Röttjers L, Fonville M, Takumi K, Takken W, Faust K, et al. Quantitative microbial population study reveals geographical differences in bacterial symbionts of Ixodes ricinus. Microbiome 2022 August;10(1):120.
32. Harris EK, Jirakanwisal K, Verhoeve VI, Fongsaran C, Suwanbongkot C, Welch MD, et al. Role of Sca2 and RickA in the Dissemination of Rickettsia parkeri in Amblyomma maculatum. Infection and immunity 2018;86:e00123–18.
33. Ireton K. Molecular mechanisms of cell-cell spread of intracellular bacterial pathogens. Open biology 2013;3:130079.
34. Merhej V, Raoult D. Rickettsial evolution in the light of comparative genomics. Biological reviews of the Cambridge Philosophical Society 2011;86:379–405.
35. Gouin E, Egile C, Dehoux P, Villiers V, Adams J, Gertler F, et al. The RickA protein of Rickettsia conorii activates the Arp2/3 complex. Nature 2004;427:457–61.
36. Bonnet SI, Pollet T. Update on the intricate tango between tick microbiomes and tick-borne pathogens. Parasite immunology 2021;43:e12813.
37. Guizzo MG, Parizi LF, Nunes RD, Schama R, Albano RM, Tirloni L, et al. A Coxiella mutualist symbiont is essential to the development of Rhipicephalus microplus. Scientific reports 2017;7:17554.
38. Duron O, Morel O, Noël V, Buysse M, Binetruy F, Lancelot R, et al. Tick-Bacteria Mutualism Depends on B Vitamin Synthesis Pathways. Current biology : CB 2018;28:1896–1902.e5.
39. Hunter DJ, Torkelson JL, Bodnar J, Mortazavi B, Laurent T, Deason J, et al. The Rickettsia Endosymbiont of Ixodes pacificus Contains All the Genes of De Novo Folate Biosynthesis. PloS one 2015;10:e0144552.
40. Gottlieb Y, Lalzar I, Klasson L. Distinctive Genome Reduction Rates Revealed by Genomic Analyses of Two Coxiella-Like Endosymbionts in Ticks. Genome biology and evolution 2015;7:1779–96.
41. Tsementzi D, Castro Gordillo J, Mahagna M, Gottlieb Y, Konstantinidis KT. Comparison of closely related, uncultivated Coxiella tick endosymbiont population genomes reveals clues about the mechanisms of symbiosis. Environmental microbiology 2018;20:1751–1764.
42. Gulia-Nuss M, Nuss AB, Meyer JM, Sonenshine DE, Roe RM, Waterhouse RM, et al. Genomic insights into the Ixodes scapularis tick vector of Lyme disease. Nature communications 2016;7:10507.
43. Miller JR, Koren S, Dilley KA, Harkins DM, Stockwell TB, Shabman RS, et al. A draft genome sequence for the Ixodes scapularis cell line, ISE6. F1000Research 2018;7:297.
44. Jia N, Wang J, Shi W, Du L, Sun Y, Zhan W, et al. Large-Scale Comparative Analyses of Tick Genomes Elucidate Their Genetic Diversity and Vector Capacities. Cell 2020;182:1328–1340.e13.
45. De S, Kingan SB, Kitsou C, Portik DM, Foor SD, Frederick JC, et al. A high-quality Ixodes scapularis genome advances tick science. Nature genetics 2023;55:301–311.
46. McClure EE, Chávez ASO, Shaw DK, Carlyon JA, Ganta RR, Noh SM, et al. Engineering of obligate intracellular bacteria: progress, challenges and paradigms. Nature reviews Microbiology 2017;15:544–558.
47. Wang T, Zhang S, Pei T, Yu Z, Liu J. Tick mitochondrial genomes: structural characteristics and phylogenetic implications. Parasites & vectors 2019;12:451.
48. Kneubehl AR, Muñoz-Leal S, Filatov S, de Klerk DG, Pienaar R, Lohmeyer KH, et al. Amplification and sequencing of entire tick mitochondrial genomes for a phylogenomic analysis. Scientific reports 2022;12:19310.
49. Ahantarig A, Trinachartvanit W, Baimai V, Grubhoffer L. Hard ticks and their bacterial endosymbionts (or would be pathogens). Folia microbiologica 2013;58:419–28.
50. Tian J, Hou X, Ge M, Xu H, Yu B, Liu J, et al. The diversity and evolutionary relationships of ticks and tick-borne bacteria collected in China. Parasites &; Vectors 2022 Oct;15(1). http://dx.doi.org/10.1186/s13071-022-05485-3.
51. Stavru F, Riemer J, Jex A, Sassera D. When bacteria meet mitochondria: The strange case of the tick symbiont Midichloria mitochondrii$^{\check{D}}$. Cellular microbiology 2020;22:e13189.
52. Ankrah NY, Luan J, Douglas AE. Cooperative metabolism in a three-partner insect-bacterial symbiosis revealed by metabolic modeling. Journal of Bacteriology 2017;199(15):10–1128.
53. Hillyard PD, et al. Ticks of north-west Europe. Field Studies Council; 1996.
54. Krawczyk AI, Bakker JW, Koenraadt CJM, Fonville M, Takumi K, Sprong H, et al. Tripartite Interactions among Ixodiphagus hookeri, Ixodes ricinus and Deer: Differential Interference with Transmission Cycles of Tick-Borne Pathogens. Pathogens 2020 Apr;9(5):339.
55. Hartemink N, van Vliet A, Sprong H, Jacobs F, Garcia-Martí I, Zurita-Milla R, et al. Temporal-Spatial Variation in Questing Tick Activity in the Netherlands: The Effect of Climatic and Habitat Factors. Vector borne and zoonotic diseases (Larchmont, NY) 2019;19:494–505.
56. Hansford KM, Fonville M, Gillingham EL, Coipan EC, Pietzsch ME, Krawczyk AI, et al. Ticks and Borrelia in urban and peri-urban green space habitats in a city in southern England. Ticks and tick-borne diseases 2017;8:353–361.
57. Heylen D, Fonville M, van Leeuwen AD, Sprong H. Co-infections and transmission dynamics in a tick-borne bacterium community exposed to songbirds. Environmental microbiology 2016;18:988–96.
58. Balraj P, El Karkouri K, Vestris G, Espinosa L, Raoult D, Renesto P. RickA expression is not sufficient to promote actin-based motility of Rickettsia raoultii. PloS one 2008;3:e2582.
59. Nijsse B, Schaap PJ, Koehorst JJ. FAIR data station for lightweight metadata management and validation of omics studies. GigaScience 2023 03;12:giad014.

60. Milhano N, Palma M, Marcili A, Núncio MS, de Carvalho IL, de Sousa R. Rickettsia lusitaniae sp. nov. isolated from the soft tick Ornithodoros erraticus (Acarina: Argasidae). Comp Immunol Microbiol Infect Dis 2014 May;37(3):189–193.
61. Ammerman NC, Beier-Sexton M, Azad AF. Laboratory maintenance of Rickettsia rickettsii. Curr Protoc Microbiol 2008 Nov;Chapter 3(1):Unit 3A.5.
62. Koehorst J, Nijsse B, n d, editor, (Hybrid) Metagenomics workflow. WorkflowHub; 2024. https://workflowhub.eu/workflows/367?version=1, accessed: 02-01-2024.
63. Goble C, Soiland-Reyes S, Bacall F, Owen S, Williams A, Eguinoa I, et al., n d, editor, Implementing FAIR Digital Objects in the EOSC-Life Workflow Collaboratory. Zenodo; 2021. https://doi.org/10.5281/zenodo.4605654.
64. Crusoe MR, Abeln S, Iosup A, Amstutz P, Chilton J, Tijanić N, et al. Methods included: standardizing computational reuse and portability with the common workflow language. Communications of the ACM 2022;65(6):54–63. https://doi.org/10.1145/3486897.
65. Amstutz P, Crusoe MR, the CWL community, n d, editor, cwltool. Zenodo; 2022. https://zenodo.org/doi/10.5281/zenodo.833999, accessed: 02-01-2024.
66. Andrews S, FastQC A quality control tool for high throughput sequence data. Babraham Bioinformatics; 2010. https://www.bioinformatics.babraham.ac.uk/projects/fastqc/.
67. Chen S, Zhou Y, Chen Y, Gu J. fastp: an ultra-fast all-in-one FASTQ preprocessor. Bioinformatics 2018;34(17):i884–i890.
68. Bushnell B. BBMap: a fast, accurate, splice-aware aligner. Lawrence Berkeley National Lab.(LBNL), Berkeley, CA (United States); 2014.
69. Li H. Minimap2: pairwise alignment for nucleotide sequences. Bioinformatics 2018;34(18):3094–3100.
70. Wood DE, Lu J, Langmead B. Improved metagenomic analysis with Kraken 2. Genome biology 2019 November;20(1):257.
71. Lu J, Breitwieser FP, Thielen P, Salzberg SL. Bracken: estimating species abundance in metagenomics data. PeerJ Computer Science 2017 Jan;3:e104.
72. Lu J, Rincon N, Wood DE, Breitwieser FP, Pockrandt C, Langmead B, et al. Metagenome analysis using the Kraken software suite. Nature protocols 2022;17(12):2815–2839.
73. Kolmogorov M, Yuan J, Lin Y, Pevzner PA. Assembly of long, error-prone reads using repeat graphs. Nature biotechnology 2019;37(5):540–546.
74. Wick RR, Holt KE. Polypolish: short-read polishing of long-read bacterial genome assemblies. PLoS computational biology 2022;18(1):e1009802.
75. Li H. Aligning sequence reads, clone sequences and assembly contigs with BWA-MEM. arXiv preprint arXiv:13033997 2013;.
76. Manni M, Berkeley MR, Seppey M, Simão FA, Zdobnov EM. BUSCO update: novel and streamlined workflows along with broader and deeper phylogenetic coverage for scoring of eukaryotic, prokaryotic, and viral genomes. Molecular biology and evolution 2021;38(10):4647–4654.
77. Nurk S, Meleshko D, Korobeynikov A, Pevzner PA. metaSPAdes: a new versatile metagenomic assembler. Genome research 2017;27(5):824–834.
78. Milne I, Milne I, Bayer M, Cardle L, Shaw P, Stephen G, et al. Tablet–next generation sequence assembly visualization. Bioinformatics (Oxford, England) 2010 February;26(3):401—402.
79. Schwengers O, Jelonek L, Dieckmann MA, Beyvers S, Blom J, Goesmann A. Bakta: rapid and standardized annotation of bacterial genomes via alignment-free sequence identification. Microbial genomics 2021;7(11):000685.
80. Huerta-Cepas J, Szklarczyk D, Heller D, Hernández-Plaza A, Forslund SK, Cook H, et al. eggNOG 5.0: a hierarchical, functionally and phylogenetically annotated orthology resource based on 5090 organisms and 2502 viruses. Nucleic acids research 2019 January;47(D1):D309—D314.
81. Kearse M, Moir R, Wilson A, Stones-Havas S, Cheung M, Sturrock S, et al. Geneious Basic: an integrated and extendable desktop software platform for the organization and analysis of sequence data. Bioinformatics 2012 Jun;28(12):1647–1649.
82. Minh BQ, Schmidt HA, Chernomor O, Schrempf D, Woodhams MD, von Haeseler A, et al. IQ-TREE 2: New models and efficient methods for phylogenetic inference in the genomic era. Mol Biol Evol 2020 May;37(5):1530–1534.
83. Kalyaanamoorthy S, Minh BQ, Wong TKF, von Haeseler A, Jermiin LS. ModelFinder: fast model selection for accurate phylogenetic estimates. Nat Methods 2017 Jun;14(6):587–589.
84. Minh BQ, Nguyen MAT, von Haeseler A. Ultrafast approximation for phylogenetic bootstrap. Mol Biol Evol 2013 May;30(5):1188–1195.
85. Guindon S, Dufayard JF, Lefort V, Anisimova M, Hordijk W, Gascuel O. New algorithms and methods to estimate maximum-likelihood phylogenies: assessing the performance of PhyML 3.0. Syst Biol 2010 May;59(3):307–321.
86. Project I, Inkscape; 2020. https://inkscape.org.
87. Minh BQ, Schmidt HA, Chernomor O, Schrempf D, Woodhams MD, von Haeseler A, et al. IQ-TREE 2: New Models and Efficient Methods for Phylogenetic Inference in the Genomic Era. Molecular biology and evolution 2020 May;37(5):1530—1534.
88. Kalyaanamoorthy S, Minh BQ, Wong TKF, von Haeseler A, Jermiin LS. ModelFinder: fast model selection for accurate phylogenetic estimates. Nature methods 2017 June;14(6):587—589.
89. Hoang DT, Chernomor O, von Haeseler A, Minh BQ, Vinh LS. UFBoot2: Improving the Ultrafast Bootstrap Approximation. Molecular biology and evolution 2018;35:518–522.
90. Machado D, Andrejev S, Tramontano M, Patil KR. Fast automated reconstruction of genome-scale metabolic models for microbial species and communities. Nucleic acids research 2018;46(15):7542–7553.
91. Lieven C, Beber ME, Olivier BG, Bergmann FT, Ataman M, Babaei P, et al. MEMOTE for standardized genome-scale metabolic model testing. Nature biotechnology 2020 March;38(3):272—276.
92. Ebrahim A, Lerman JA, Palsson BO, Hyduke DR. COBRApy: constraints-based reconstruction and analysis for python. BMC systems biology 2013;7:1–6.
93. Rozas J, Ferrer-Mata A, Sánchez-DelBarrio JC, Guirao-Rico S, Librado P, Ramos-Onsins SE, et al. DnaSP 6: DNA Sequence Polymorphism analysis of large data sets. Mol Biol Evol 2017 Dec;34(12):3299–3302.
94. Oksanen J, Simpson GL, Blanchet FG, Kindt R, Legendre P, Minchin PR, et al., vegan: Community Ecology Package; 2023. https://github.com/vegandevs/vegan, r package version 2.6-5.
95. Sayers EW, Bolton EE, Brister JR, Canese K, Chan J, Comeau DC, et al. Database resources of the national center for biotechnology information. Nucleic acids research 2022 January;50(D1):D20—D26.
96. Azagi T, Dirks RP, Yebra-Pimentel ES, Schaap PJ, Koehorst JJ, Esser HJ, et al. Assembly and Comparison of Neoehrlichia mikurensis Genomes. Microorganisms 2022 May;10(6):1134.
97. Garcia-Vozmediano A, Tomassone L, Fonville M, Bertolotti L, Heylen D, Fabri ND, et al. The Genetic Diversity of Rickettsiella Symbionts in Ixodes ricinus Throughout Europe. Microbial ecology 2022 August;84(2):613—626.
98. Jain C, Rodriguez-R LM, Phillippy AM, Konstantinidis KT, Aluru S. High throughput ANI analysis of 90K prokaryotic genomes reveals clear species boundaries. Nature communications 2018 November;9(1):5114.
99. Carpi G, Kitchen A, Kim HL, Ratan A, Drautz-Moses DI, McGraw JJ, et al. Mitogenomes reveal diversity of the European Lyme borreliosis vector Ixodes ricinus in Italy. Mol Phylogenet Evol 2016 Aug;101:194–202.
100. Sassera D, Lo N, Epis S, D'Auria G, Montagna M, Comanda-

tore F, et al. Phylogenomic evidence for the presence of a flagellum and cbb(3) oxidase in the free-living mitochondrial ancestor. Molecular biology and evolution 2011 December;28(12):3285—3296.
101. Dong X, El Karkouri K, Robert C, Gavory F, Raoult D, Fournier PE. Genomic comparison of Rickettsia helvetica and other Rickettsia species. Journal of bacteriology 2012 May;194(10):2751.
102. Helminiak L, Mishra S, Kim HK. Pathogenicity and virulence of Rickettsia. Virulence 2022 December;13(1):1752—1771.
103. Ronai I, de Paula Baptista R, Paulat NS, Frederick JC, Azagi T, Bakker JW, et al. The repetitive genome of the Ixodes ricinus tick reveals transposable elements have driven genome evolution in ticks. bioRxiv 2024;https://www.biorxiv.org/content/early/2024/03/14/2024.03.13.584159.
104. Wiesinger A, Wenderlein J, Ulrich S, Hiereth S, Chitimia-Dobler L, Straubinger RK. Revealing the Tick Microbiome: Insights into Midgut and Salivary Gland Microbiota of Female Ixodes ricinus Ticks. International journal of molecular sciences 2023 January;24(2):1100.
105. Coipan EC, Jahfari S, Fonville M, Maassen CB, van der Giessen J, Takken W, et al. Spatiotemporal dynamics of emerging pathogens in questing Ixodes ricinus. Frontiers in cellular and infection microbiology 2013;3:36.
106. Kagemann J, Clay K. Effects of infection by Arsenophonus and Rickettsia bacteria on the locomotive ability of the ticks Amblyomma americanum, Dermacentor variabilis, and Ixodes scapularis. Journal of medical entomology 2013 January;50(1):155—162.
107. Maitre A, Wu-Chuang A, Mateos-Hernández L, Foucault-Simonin A, Moutailler S, Paoli JC, et al. Rickettsia helvetica infection is associated with microbiome modulation in Ixodes ricinus collected from humans in Serbia. Scientific reports 2022 July;12(1):11464.
108. Reed SCO, Lamason RL, Risca VI, Abernathy E, Welch MD. Rickettsia actin-based motility occurs in distinct phases mediated by different actin nucleators. Current biology : CB 2014 January;24(1):98—103.
109. Haglund CM, Choe JE, Skau CT, Kovar DR, Welch MD. Rickettsia Sca2 is a bacterial formin-like mediator of actin-based motility. Nature cell biology 2010 November;12(11):1057—1063.
110. Oliver JD, Burkhardt NY, Felsheim RF, Kurtti TJ, Munderloh UG. Motility characteristics are altered for Rickettsia bellii transformed to overexpress a heterologous rickA gene. Applied and environmental microbiology 2014 February;80(3):1170—1176.
111. Sallay B, Vaculova T, Derdakova M, Špitalská, E and Škultéty, L' and others. Two mice models for transferability of zoonotic bacteria via tick vector. Acta virologica 2017;61(3):372–376.
112. Burgdorfer W, Aeschlimann A, Peter O, Hayes SF, Philip RN. Ixodes ricinus: vector of a hitherto undescribed spotted fever group agent in Switzerland. Acta tropica 1979;36:357–67.
113. Watanabe K, Yukuhiro F, Matsuura Y, Fukatsu T, Noda H. Intrasperm vertical symbiont transmission. Proceedings of the National Academy of Sciences of the United States of America 2014 May;111(20):7433—7437.
114. Hurst L. Parasite diversity and the evolution of diploidy, multicellularity and anisogamy. Journal of theoretical biology 1990 June;144(4):429—443.
115. Wang M, Zhu D, Dai J, Zhong Z, Zhang Y, Wang J. Tissue Localization and Variation of Major Symbionts in Haemaphysalis longicornis, Rhipicephalus haemaphysaloides, and Dermacentor silvarum in China. Applied and environmental microbiology 2018 May;84(10):e00029—18.
116. Hayes S, Burgdorfer W, Aeschlimann A. Sexual transmission of spotted fever group rickettsiae by infected male ticks: detection of rickettsiae in immature spermatozoa of Ixodes ricinus. Infection and immunity 1980 February;27(2):638—642.
117. Beninati T, Lo N, Sacchi L, Genchi C, Noda H, Bandi C. A novel alpha-Proteobacterium resides in the mitochondria of ovarian cells of the tick Ixodes ricinus. Applied and environmental microbiology 2004 May;70(5):2596—2602.
118. Di Venere M, Fumagalli M, Cafiso A, De Marco L, Epis S, Plantard O, et al. Ixodes ricinus and Its Endosymbiont Midichloria mitochondrii: A Comparative Proteomic Analysis of Salivary Glands and Ovaries. PloS one 2015;10(9):e0138842.
119. Guizzo MG, Hatalová T, Frantová H, Zurek L, Kopáček P, Perner J. Ixodes ricinus ticks have a functional association with Midichloria mitochondrii. Frontiers in cellular and infection microbiology 2022;12:1081666.
120. Mariconti M, Epis S, Sacchi L, Biggiogera M, Sassera D, Genchi M, et al. A study on the presence of flagella in the order Rickettsiales: the case of 'Candidatus Midichloria mitochondrii'. Microbiology 2012 Jul;158(Pt 7):1677–1683.
121. Olivieri E, Epis S, Castelli M, Varotto Boccazzi I, Romeo C, Desirò A, et al. Tissue tropism and metabolic pathways of Midichloria mitochondrii suggest tissue-specific functions in the symbiosis with Ixodes ricinus. Ticks Tick Borne Dis 2019 Aug;10(5):1070–1077.
122. Gu C, Kim GB, Kim WJ, Kim HU, Lee SY. Current status and applications of genome-scale metabolic models. Genome Biol 2019 Jun;20(1):121.
123. Andersson S, Zomorodipour A, Andersson J, Sicheritz-Pontén T, Alsmark U, Podowski R, et al. The genome sequence of Rickettsia prowazekii and the origin of mitochondria. Nature 1998 November;396(6707):133—140. https://www.nature.com/articles/24094.pdf.
124. Walker DH, Yu XJ. Progress in rickettsial genome analysis from pioneering of Rickettsia prowazekii to the recent Rickettsia typhi. Annals of the New York Academy of Sciences 2005 December;1063:13—25. https://doi.org/10.1196/annals.1355.003.
125. Renesto P, Ogata H, Audic S, Claverie JM, Raoult D. Some lessons from Rickettsia genomics. FEMS microbiology reviews 2005;29(1):99–117.
126. Price DR, Bartley K, Blake DP, Karp-Tatham E, Nunn F, Burgess ST, et al. A Rickettsiella endosymbiont is a potential source of essential B-vitamins for the poultry red mite, Dermanyssus gallinae. Frontiers in Microbiology 2021;12:695346.
127. Olivieri E, Epis S, Castelli M, Boccazzi IV, Romeo C, Desirò A, et al. Tissue tropism and metabolic pathways of Midichloria mitochondrii suggest tissue-specific functions in the symbiosis with Ixodes ricinus. Ticks and tick-borne diseases 2019;10(5):1070–1077.
128. Buysse M, Floriano AM, Gottlieb Y, Nardi T, Comandatore F, Olivieri E, et al. A dual endosymbiosis supports nutritional adaptation to hematophagy in the invasive tick Hyalomma marginatum. Elife 2021;10:e72747.
129. BioModels, Biomodels;. https://www.ebi.ac.uk/biomodels/curation/fbc.